Aus der Klinik für Neurologie mit Experimentellen Neurologie
der Medizinischen Fakultät Charité – Universitätsmedizin Berlin

DISSERTATION

Connectomic Targets für die Tiefenhirnstimulation
Connectomic Targets for Deep Brain Stimulation

zur Erlangung des akademischen Grades
Doctor rerum medicinalium (Dr. rer. medic.)

vorgelegt der Medizinischen Fakultät
Charité – Universitätsmedizin Berlin

von

Ningfei Li

aus Shaanxi, China

Datum der Promotion: 25. November 2022

Table of Contents

List of Abbreviations I
Abstract III
Zusammenfassung V
1. Introduction 1
2. Methods 4
2.1 Patient Cohorts and Imaging 4
2.2 Lead Localization and VTA Estimation 5
2.3 Structural Connectivity Analysis 6
3. Results 9
3.1 Intra-cohort Analysis 9
3.2 Inter-cohort Cross-prediction 9
3.3 Replication on Independent Test Cohorts 10
3.4 A connectomic target for OCD-DBS 12
4. Discussion 14
4.1 A unifying tract target for DBS in OCD 14
4.2 Toward symptom-specific circuitopathies 15
4.3 Limitations 16
4.4 Conclusions 18
References 19
Statutory Declaration 33
Extract from the Journal Summary List 35
Publication 37
Curriculum Vitae 49
Acknowledgements 53

List of Abbreviations

DBS	Deep Brain Stimulation
PD	Parkinson's Disease
OCD	Obsessive Compulsive Disorder
slMFB	Supero-lateral branch of the Medial Forebrain Bundle
ALIC	Anterior Limb of the Internal Capsule
vALIC	Ventral Anterior Limb of the Internal Capsule
MRI	Magnetic Resonance Imaging
fMRI	Functional Magnetic Resonance Imaging
dMRI	Diffusion Magnetic Resonance Imaging
STN	Subthalamic Nucleus
NAcc	Nucleus Accumbens
VC/VS	Ventral Capsule/Ventral Striatum
ITP	Inferior Thalamic Peduncle
BNST	Bed Nucleus of the Stria Terminalis
amGPi	Anteromedial Globus Pallidus interna
MD/V ANT	Medial Dorsal/Ventral Anterior Nucleus of the Thalamus
Y-BOCS	Yale-Brown Obsessive-Compulsive Scale
CT	Computer Tomography
VTA	Volumes of Tissue Activated
ANTs	Advanced Normalization Tools
MNI	Montreal Neurological Institute
SyN	Symmetric Normalization
FEM	Finite Element Method
HCP	Human Connectome Project
MD	Mediodorsal
PFC	Prefrontal Cortex
dACC	Dorsal Anterior Cingulate Cortex
vlPFC	Ventrolateral Prefrontal Cortex
CSTC	Cortico-Striato-Thalamo-Cortical

M1	Primary Motor Cortex
SMA	Supplementary Motor Area

Abstract

Deep brain stimulation (DBS), a highly effective and well-established treatment option for movement disorders, is now also used to treat psychiatric disorders, such as obsessive-compulsive disorder (OCD) or major depression. A variety of surgical targets for DBS have been proposed not only for different diseases but also for the same disease. However, different targets may potentially lie within the same brain network or even alongside the same fiber bundle which is responsible for clinical improvement. Within the scope of this study, we hence investigated whether different stimulation sites would modulate one common tract target mediating beneficial OCD outcome. Specifically, four cohorts of OCD patients that underwent DBS to either the anterior limb of the internal capsule (ALIC) or the subthalamic nucleus (STN) were analyzed using a connectomic approach. Fiber tracts that were associated with clinical improvement – based on the Yale-Brown Obsessive-Compulsive Scale (Y-BOCS) – were isolated, assigned with predictive values and visualized. The same fronto-subcortical fiber tract that was positively discriminative of good clinical outcome emerged for both target-specific cohorts. Moreover, the tract derived from data of the ALIC-cohort was predictive of clinical improvement in the STN-cohort and vice versa.

The results suggest that modulating a specific fronto-subthalamic fiber bundle may represent an important unifying substrate for improving global obsessive-compulsive behavior in OCD across different stimulation sites. In synergy, the study advances the concept of connectomic deep brain stimulation above and beyond OCD, showing for the first time that a connectivity-derived model could potentially facilitate defining the connectomic target for DBS.

Zusammenfassung

Die Tiefe Hirnstimulation (DBS), eine hochwirksame und etablierte Behandlungsoption bei Bewegungsstörungen, wird mittlerweile auch bei psychiatrischen Erkrankungen wie Zwangsstörungen (OCD) oder schweren Depressionen eingesetzt. Mehrere chirurgische Ziele für die DBS existieren nicht nur für verschiedene Krankheiten, sondern teilweise auch für dieselbe Krankheit. Möglicherweise liegen jedoch unterschiedliche Ziele innerhalb eines selben Gehirnnetzwerks oder sogar innerhalb desselben Faserbündels, welches für die klinische Verbesserung verantwortlich ist. Im Rahmen dieser Studie untersuchten wir daher, ob verschiedene Stimulationsorte einen gemeinsamen Trakt modulieren, welcher ein vorteilhaftes klinisches OCD-Ergebnis vermittelt.

Konkret wurden vier Kohorten von Patienten mit einer Zwangsstörung, bei welchen die Implantation einer DBS entweder an dem vorderen Teil der Capsula interna (ALIC) oder am Nucleus subthalamicus (STN) durchgeführt wurde, unter Benutzung eines strukturellen Konnektoms analysiert. Fasertrakte, die mit einer klinischen Verbesserung assoziiert waren – basierend auf der Yale-Brown Obsessive-Compulsive Scale (Y-BOCS) – wurden isoliert, mit prädiktiven Werten belegt und visualisiert. Für beide zielspezifische Kohorten trat der gleiche fronto-subkortikale Fasertrakt auf, der mit einem guten klinischen Ergebnis assoziiert war. Darüber hinaus war der aus den Daten der ALIC-Kohorte abgeleitete Trakt prädiktiv für eine klinische Verbesserung in der STN-Kohorte und umgekehrt.

Die Ergebnisse legen nahe, dass die Modulation eines spezifischen fronto-subthalamischen Faserbündels ein wichtiges verbindendes Substrat zur Verbesserung des Zwangsverhaltens bei Zwangsstörungen über verschiedene Stimulationsorte hinweg darstellen kann. In Synergie entwickelt diese Studie das Konzept der konnektomischen Tiefenhirnstimulation über die Zwangsstörung hinaus und zeigt erstmalig, dass ein von der Konnektivität abgeleitetes Modell möglicherweise die Definition eines konnektomischen Ziels für die DBS erleichtern könnte.

1. Introduction

Deep Brain Stimulation (DBS), as a highly effective neuromodulation treatment option, has been widely used to treat movement disorders such as Parkinson's disease (PD), dystonia, essential tremor, and Tourette syndrome. More recently, DBS has also been investigated and applied to other brain diseases such as epilepsy, depression, Alzheimer's disease, and OCD. With the increasing numbers of indications, a variety of stimulation targets have been proposed – even within the same disease.

In the meantime, DBS has been experiencing a conceptual paradigm shift away from stimulating specific focal brain nuclei toward modulating distributed brain networks that span across the whole scale of the human brain [1–3]. Within the framework of this emerging field of connectomic DBS, it has been discussed whether some or most of the proposed neurosurgical targets may in fact modulate the same brain network. As an initial hint toward the tenability of such concept, Schlaepfer et al. showed in a pilot study that DBS to the supero-lateral branch of the medial forebrain bundle (slMFB), which entertains close connections to most if not all neurosurgical targets previously proposed for depression, is efficacious in treating highly refractory depression [4]. Along similar lines, a recent study demonstrated for the case of OCD that the distance between slMFB and the active DBS contacts was associated with clinical improvements in OCD patients receiving DBS to the ventral anterior limb of the internal capsule (vALIC), even though the location of the active contacts itself was not related the treatment response [5].

These initial studies raise the possibility that a white matter fiber tract could be modulated in similar fashion when targeted via different vantage points along its anatomical course. In other words, the tract itself could serve as a potential surgical target. Such a concept might be oversimplified given the complexity of the human brain and each structure's function. Nevertheless, older invasive treatments like cingulotomy and capsulotomy primarily attempted to disrupt frontal connections by lesioning white matter bundles [6]. Moreover, for PD, it was recently shown that network-based concepts could be predictive of clinical outcome across DBS centers [2].

In parallel, following developments in the field of neuroimaging, the term of "connectome" was introduced in 2005 [7]. As a formal way of analyzing whole-brain networks, the introduction of the human brain connectome opened an opportunity for many applications and has had enormous impact on the field. Using state-of-the-art

neuroimaging methods and high-resolution connectomes, it has been demonstrated that connectivity of the DBS electrodes to specific cortical regions is associated with the clinical outcome in various diseases [2,8–11].

The combination of connectomics and DBS resulted in a connectomic approach to surgery, which was introduced by Jaimie Henderson in 2012 [12]. In the article, Henderson proposed that connectomic surgery, which focuses on modulating large scale networks instead of stimulating focal brain regions, could provide a potential therapy for patients in minimally conscious state. Over the last decade, DBS targeting has become more and more precise with the development and increasing application of connectomic data such as diffusion Magnetic Resonance Imaging (dMRI) and functional Magnetic Resonance Imaging (fMRI). In this dissertation study, we investigated the definition of connectomic targets based on normative connectomes, specifically in DBS for OCD [13].

OCD is a common, long-lasting psychiatric disorder with a lifetime prevalence of 2.3% [14]. About 10% of OCD patients are deemed refractory to conventional first-line treatments. Treatment of severe OCD by DBS targeting the anterior limb of the internal capsule (ALIC) has been approved by the U.S. Food and Drug Administration (Humanitarian Device Exemption) in 2009. A variety of other targets have also been proposed since then, including the subthalamic nucleus (STN) [15,16], nucleus accumbens (NAcc) [17–19], ventral capsule/ventral striatum (VC/VS) [20], inferior thalamic peduncle (ITP) [21,22], bed nucleus of the stria terminalis (BNST) [23], anteromedial globus pallidus interna (amGPi) [24], superolateral branch of the medial forebrain bundle (slMFB) [25] and medial dorsal and ventral anterior nucleus of the thalamus (MD/V ANT) [26] (see [27] for an overview of anatomical targets). Moreover, applying stimulation to a combination of different targets has been proposed as a potential strategy. For example, a recent prospective clinical trial implanted four electrodes per patient, with one pair in the STN and one in the ALIC [28].

From a connectomic perspective, stimulation of different anatomical targets may indeed modulate the same network responsible for clinical outcome. A previous study by Baldermann et al. showed that structural connectivity between DBS electrodes and medial and lateral prefrontal cortices was associated with clinical improvement [8]. Specifically, a fiber bundle passing through the ventral ALIC was found to be predictive of clinical improvement after one year of DBS and connectivity to this fiber tract explained ~40 % of the variance in clinical outcome. This specific fiber tract connected to both the anterior part of the STN and the medial dorsal nucleus of the thalamus. The STN itself is

a widely used DBS target for various diseases including PD [29], dystonia [30], Tourette's Syndrome [31], and OCD [32]. It receives afferents from most parts of the prefrontal cortex and is involved in the processing of motor, associative and limbic information [33]. Owing to the profile of its cortico-subthalamic projections, the STN can be subdivided into different functional regions in analogy to the organization of the frontal cortex. The anterior (associative/limbic) parts of the STN, which have served as DBS targets for OCD [32], were also connected to the fiber bundle identified by Baldermann et al. in ALIC-DBS patients [8]. In another study by Tyagi et al. [28], in which both anteromedial STN and VC/VS were targeted, it was shown that stimulation at both sites could significantly and equally alleviated OCD symptoms, while STN-DBS preferentially improved cognitive flexibility and VC-DBS had more effect on mood.

Building on these findings, in this dissertation study, four cohorts of DBS patients that received either STN-DBS or ALIC-DBS were retrospectively analyzed using a connectome-based approach. The aim of the study is not only to test our hypothesis that the same fiber tract could potentially be predictive of the clinical improvement in both STN-DBS and ALIC-DBS, but also to establish the methodology to define the connectomic-target for DBS.

2. Methods

2.1 Patient Cohorts and Imaging

Retrospective data of 36 OCD patients from two centers were initially enrolled in this study [34], comprising Cologne (N = 22, ALIC-DBS patients) and Grenoble (N = 14, STN-DBS patients) cohorts. Two additional cohorts of 14 OCD patients were further used for validation, including Madrid (N = 8, NAcc-DBS patients) and London cohorts (N = 6, patients received bilateral electrodes to both STN and ALIC). Since, on average, placement of electrodes implanted to the NAcc is comparable to the one of electrodes implanted to the ALIC, we subsumed electrodes of patients from Madrid as part of the ALIC zone cohort. All patients from Cologne and Grenoble cohorts were bilaterally implanted with DBS electrodes of the Medtronic 3389 type, except for three patients from the Cologne cohort, who received Medtronic 3387 type electrodes (Medtronic, Minneapolis, Minnesota, US). Patients from Madrid cohort were implanted with Medtronic 3391 electrodes. Patients from the London cohort received Medtronic 3389 type electrodes to the STN and Medtronic 3387 type electrodes to the ALIC. All patients were eligible for DBS based on their diagnoses of treatment-refractory, severe OCD [8,32].

Pre- and postoperative severity of OCD was assessed based on the Yale-Brown Obsessive-Compulsive Scale (Y-BOCS). For Cologne, Grenoble, and London cohorts, postoperative Y-BOCS score were obtained 12 months after surgery. For the Madrid cohort, each of the four contact pairs was activated for a duration of three months, together with a one-month washout period and a three-month sham period, which resulted in 32 improvement scores in our analysis. Detailed demographic data of the four cohorts are shown in Table 1 (adapted from [13]). All patients gave written informed consent. Study protocols were approved by each local Ethics Committee.

Table 1: Patient demographic details and clinical results of the four cohorts (adapted from [13])

	ALIC DBS Cohort (Mean ± SD)	STN DBS Cohort (Mean ± SD)	NAcc DBS Cohort (Mean ± SD)	Combined DBS Cohort (Mean ± SD)
Center	University Hospital Cologne	University Hospital Grenoble	Hospital Clínico San Carlos Madrid	University Hospital London
Reference(s)	([8,35])	(32)	([36])	(28)
N patients (females)	22 (12)	14 (9)	8 (4)	6 (1)
N electrodes	44	28	16	24
Age	41.7 ± 20.5	41 ± 9	35.3 ± 10.4	45.5 ± 10.5
Y-BOCS Baseline	31.3 ± 4.4	33.4 ± 3.7	30 ± 7.75	36.2 ± 1.8
Y-BOCS after DBS	20.7 ± 7.7 *(12 months postop)*	19.6 ± 10.6 *(12 months postop)*	14.75 ± 7.2 *(3 months postop of best contact)*	14.3 ± 4.1 *(optimized phase in [16])*
Absolute Y-BOCS Improvement	9.6 ± 6.5	13.8 ± 10.8	15.1 ± 9.6	21.83 ± 5.7
% Y-BOCS Improvement	31.0 ± 20.5 %	41.2 ± 31.7 %	47.8 ± 23	60.2 ± 12.7 %

ALIC, anterior limb of the internal capsule; DBS, deep brain stimulation; NAcc, nucleus accumbens; STN, subthalamic nucleus; Y-BOCS, Yale-Brown Obsessive Compulsive Scale.

For all patients, preoperative high-resolution structural T1-weighted MRI were acquired on a 3.0-Tesla MRI-scanner. Postoperatively, computer tomography (CT) was obtained in thirty-three patients to evaluate lead electrode placement, while eleven patients from the Grenoble cohort and six London patients received postoperative MRI instead.

2.2 Lead Localization and VTA Estimation

DBS electrodes localization and Volumes of Tissue Activated (VTA) estimation were performed using default settings in Lead-DBS software (https://www.lead-dbs.org) [37,38]. Lead-DBS is a MATLAB-based open-source toolbox for DBS neuroimaging analysis which is built in the lab, and I have been one of the core contributors of it (https://github.com/netstim/leaddbs/graphs/contributors). The toolbox has been validated and widely used in the DBS world (https://www.lead-dbs.org/about/publications/). A detailed overview of the pipeline was shown in [38]. The main processing steps are described as follows.

First, postoperative CT or MRI scans were linearly coregistered to preoperative structural T1 images using Advanced Normalization Tools (ANTs; https://github.com/ANTsX/ANTs)

[39]. Since air may enter the skull during surgery, nonlinear deformation of the brain may arise with respect to the skull (termed brain shift). Thus, the coregistration was further corrected for brain shift using a three-fold linear registration as implemented in Lead-DBS software. Images were then normalized into ICBM 2009b Nonlinear Asymmetric MNI (Montreal Neurological Institute) template [40] space using the SyN (Symmetric Normalization) algorithm implemented in ANTs [41], with an additional subcortical refinement stage to ensure the most precise alignment of subcortical regions ("Effective Low Variance" preset + Subcortical Refinement option as implemented in Lead-DBS). This specific method emerged as top performer for subcortical normalization in a recent comparative study that involved >11,000 nonlinear warps in >100 subjects and investigated a variety of modern algorithms [42]. Both coregistration and normalization results were visually reviewed and refined if needed.

DBS electrodes were then pre-localized in patients' native space using either the PaCER [43] algorithm (in case of postoperative CT), or the TRAC/CORE [37] algorithm (in case of postoperative MRI). Automatic pre-localization results were reviewed and manually refined if needed. Subsequently, native space localizations were warped into MNI space using the transformations from the image normalization step.

Volumes of Tissue Activated (VTA) were estimated in native space based on patient-specific stimulation parameters, using an Finite Element Method (FEM)-based approach as described in [38]. First, volumetric meshes were constructed for gray matter (defined by subcortical brain atlases), white matter, lead contacts and insulating parts, respectively. The electric field (E-field) distribution was then estimated in the four-compartment finite element model using an adaptation of the FieldTrip-SimBio pipeline [44] integrated into Lead-DBS (http://fieldtriptoolbox.org; https://www.mrt.uni-jena.de/simbio;). A threshold at the level of 0.2 V/m [38] was applied to create binary VTAs.

2.3 Structural Connectivity Analysis

Structural connectivity in our analyses was defined on the basis of a normative connectome, which had been informed on diffusion imaging data of 985 healthy participants scanned within the framework of the Human Connectome Project (HCP) 1200 Subjects Data Release [45]. To calculate this connectome, whole brain fiber tractography was performed for each subject in the normative data set. First, fiber tracts were mapped into standard MNI space. Second, a set of 6000 fibers were sampled from

each subject and then aggregated to form the final connectome of ~6,000,000 tracts used for the analysis in this study.

In a next step, one structural connectivity profile was calculated for each patient based on the previously calculated normative connectome by seeding from patient-specific VTAs in a similar approach as described in previous work [2,8,38,46–48]. On a tract-by-tract basis, such patients with VTAs connected to the respective tract were first divided from such patients with unconnected VTAs. Second, a "Fiber *t*-score" was assigned to each tract by statistically comparing Y-BOCS change scores between the two patient groups in form of two sample *t*-tests (Figure 1, as reproduced from [13], panel B). *T*-values resulting from these comparisons were then used to define the fiber *T*-scores. Since *t*-tests were two-sided, fiber *T*-scores could be either positive or negative. Additionally, a high absolute value of the *T*-score indicated that the fiber's connection status to the VTAs was strongly discriminative (or predictive) for clinical improvements. Consequently, a high positive *T*-score meant that patients would be likely to gain clinical benefit from the stimulation if their VTAs were connected to the fiber tract. Repeating this procedure across the normative connectome resulted in a model of optimal electrode connectedness associated with maximal improvement in global obsessive-compulsive symptomatology. The above-described approach is illustrated in Figure 1 (reproduced from [13]). The structural connectivity analysis was performed using Fiber Filtering Explorer, which is part of the Lead-DBS toolbox.

For the purpose of this study, only the top 20% of predictive fibers (based on the absolute values of fiber *T*-scores) were retained to form the "discriminative fiber set". Associations between fiber connectivity and clinical improvements were then evaluated based on the discriminative fiber set. In subsequent analyses, we performed intra-cohort as well as inter-cohort prediction tests. More precisely, a discriminative fiber set was defined exclusively on one cohort but used for the prediction of clinical outcomes of patients from another cohort. Specifically, *T*-scores of connected fibers of each patient were summed and correlated with relative clinical improvements, as calculated via the difference between preoperative and postoperative Y-BOCS total scores at 12-month follow-up. Of note, since larger VTAs (due to stimulations of higher amplitudes) may connect to more fibers and, thus, may potentially automatically display higher fiber *T*-scores, we divided the scores each patient received by the stimulation amplitude. For the correlation analysis, Monte-Carlo permutation (N=1000) was performed to obtain the p-

value. This procedure is assumption-free and hence suitable for small sample sizes.

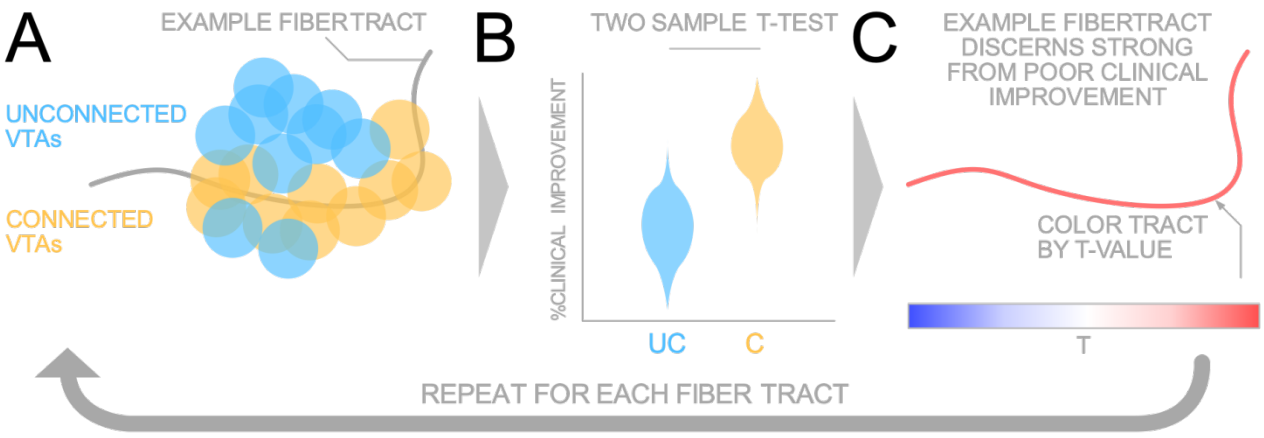

Figure 1. Summary of method to calculate fiber *T*-score. A) For each fiber tract in the normative connectome, patients were divided into two groups as a function of the connection status of their volumes of tissue activated (VTAs) (i.e., depending on whether their VTAs were connected [C; yellow] or unconnected [UC; blue)] with the respective fiber tract). B) Two-sample *t*-tests between clinical improvements of patients with connected and unconnected VTAs were calculated for each fiber tract. C) The resulting *T*-values were assigned to each fiber as an indication of its *discernibility* for good/poor clinical outcome. Fiber T scores were color-coded in a way that red coded for the fiber tract being positively connected to top responders while blue meant the opposite. Reproduced from [13].

3. Results

Age, Y-BOCS score baseline and improvements were comparable across all four cohorts (see Table 1 for demographic details). Accurate lead placement was confirmed for all patients via electrode localization using Lead-DBS (see Figure 1 in [13]).

3.1 Intra-cohort Analysis

For connectivity analysis, we first calculated one set of predictive fibers for the Cologne cohort (ALIC target) and the Grenoble cohort (STN target) separately based on the HCP normative connectome. Connected fibers (without weighing tracts for clinical outcome), predictive fibers, and intra-cohort leave-nothing-out prediction results are shown in Figure 2 (reproduced from [13]). Since the ALIC serves as a white matter target while the STN is the main entry point of basal ganglia, the overall connectivity pattern from active contacts (VTAs) to other brain regions was very different between the two cohorts (Figure 2, as reproduced from [13], top row). However, when weighing the connected fiber tracts via the *T*-score method described above, a common positively discriminative tract could be identified which connected to the medial prefrontal cortex bilaterally and was shared by both cohorts (Figure 2 in [13], middle row). The intra-cohort prediction tests showed that sum of aggregated fiber *T*-scores for each patient was highly correlated with empirical clinical improvement ($R = 0.63$ at $p < 0.001$ in the ALIC cohort; $R = 0.77$ at $p < 0.001$ in the STN cohort; Figure 2, as reproduced from [13], bottom row).

3.2 Inter-cohort Cross-prediction

While according to the intra-cohort result, discriminative fiber tracts showed good ability of explaining clinical outcome of patients within the respective cohort used to inform the model (i.e., when performing in-sample predictions), we were further interested in its capacity of predicting out-of-sample data (i.e., when performing inter-cohort cross-prediction). Therefore, in the next step, we calculated the discriminative fiber tracts solely based on the ALIC cohort and then used these to predict clinical outcome of the STN cohort ($R = 0.49$ at $p = 0.041$; Figure 2, as reproduced from [13], top row), and vice versa ($R = 0.50$ at $p < 0.009$; Figure 2, as reproduced from [13], bottom row). Of note, for some patients from the ALIC cohort, their VTAs were located entirely below the identified fiber tract and thus received near-zero fiber *T*-scores (Figure 2, as reproduced from [13], bottom row left). We further ran a two-sample *t*-test between Y-BOCS improvements of these

patients and other patients whose VTAs showed high overlap with the tract (i.e., such tracts assigned with aggregated *T*-scores > 50). Our results showed that patients with VTAs largely overlapping the tract had significantly better clinical outcome ($T = 6.0$ at $p < 10^{-5}$ when the tract was calculated based on the data from the ALIC cohort itself ($T = 3.7$ at $p < 0.005$) than when the tract was derived from data of the STN cohort.

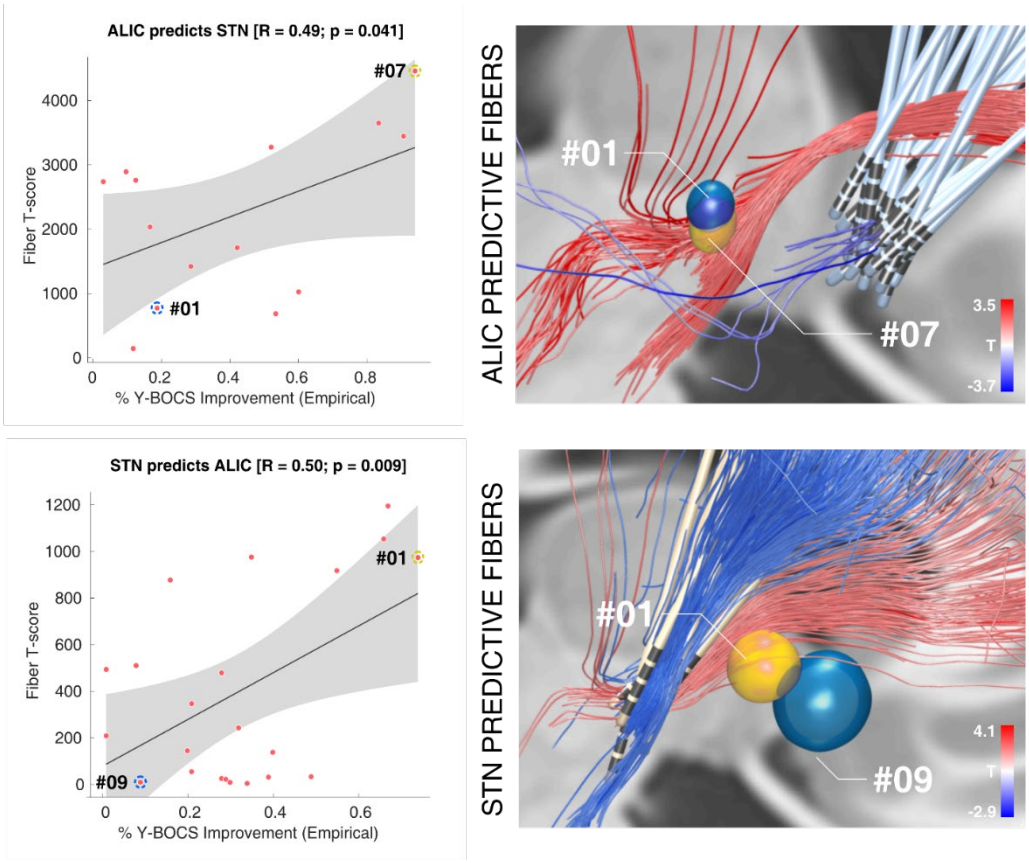

Figure 2. Cross-prediction between anterior limb of the internal capsule (ALIC) and subthalamic nucleus (STN) cohorts. Top: One set of discriminative fiber tracts was calculated based on data from the ALIC cohort and used to calculate aggregated fiber *T*-scores for patients in the STN cohort, which correlated with clinical improvements in the STN cohort. One example patient whose volume of tissue activated (VTA) (yellow) largely overlapped the tract received a high Fiber *T*-score, whereas one with less overlap (blue) received a lower score. The two example patients are also highlighted in the correlation plot on the left. Bottom: the tract was calculated exclusively on data from the STN cohort and used to predict outcome for patients in the ALIC cohort. Again, two example patients whose VTA is in a different relative location to the discriminative fiber tract are shown. Reproduced from [13].

3.3 Replication on Independent Test Cohorts

We performed the same analysis on Cologne and Grenoble cohorts combined in the next step. The same discriminative tract emerged again and even in more pronounced fashion (Figure 3, as reproduced from [13], top). Here, the positive discriminative fiber bundle which

was able to differentiate well between top and poor responders is displayed in red color. The tract coursed centrally or slightly ventrally to the electrodes of the STN cohort and passed slightly dorsally to the electrodes of the ALIC cohort. VTAs of patients with good improvement were prone to be connected to the tract, while non- or poor responders' VTAs tended to be unconnected or only slightly overlapped the tract.

To further verify if the identified discriminative fiber tract could explain the clinical improvement of out-sample data, it was used to predict the outcome of independent test cohorts from two additional centers (Madrid and London). As described in the Method section, for patients in the Madrid cohort ($N = 8$), each contact pair had been switched on for three months. Therefore, we obtained 32 data points in total (Figure 3, as reproduced from [13], bottom row left, data point color coded by active contact). For the London cohort ($N = 6$), each patient received four electrodes (two to each target). A fiber T-score was calculated for each patient by summing scores across targets. Results of the replication test are shown in Figure 3 (reproduced from [13]) bottom row. The aggregated fiber T-scores correlated with clinical improvements in both cohorts ($R = 0.50$ at $p < 0.001$ for the Madrid

cohort; R = 0.75 at p =0.040 for the London cohort).

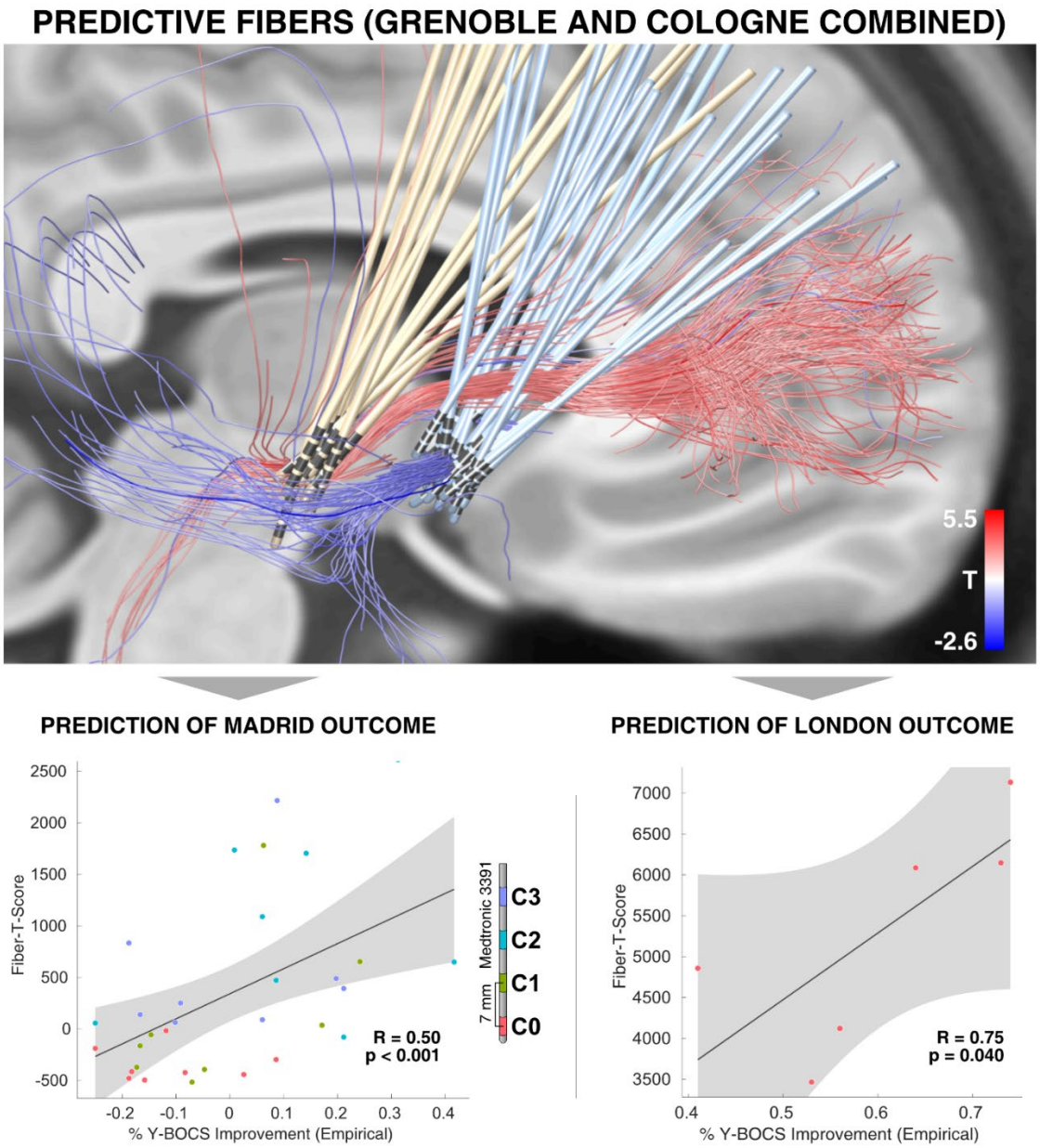

Figure 3. Predictions in independent test cohorts. Top: predictive fiber tract calculated on Cologne and Grenoble cohorts combined. Red fibers are positively correlated with clinical improvement, while blue fibers are negatively correlated. Bottom: sum of fiber T-scores under each patient's VTA predicted %-Y-BOCS improvements of the Madrid cohort (left) and the London cohort (right). Reproduced from [13].

3.4 A connectomic target for OCD-DBS

The final bundle we identified here may be seen as a "tract-target", which has the potential to "unify" the STN and ALIC targets for DBS treatment of OCD. Therefore, in a final analysis, we tried to embed the tract into the larger context of other DBS targets that

have previously been employed to treat OCD. Specifically, we extracted the target coordinates from relevant literature (Table 2 in [13]), converted them into template (MNI) space in a probabilistic fashion [47], and then overlayed them alongside the tract target (Figure 5a and 5b in [13]). Most literature-derived DBS targets for OCD concentrated closely around the tract target. Moreover, we found that the overlap between reported target sites weighted by fiber T-scores and the identified tract was highly correlated with the reported average clinical improvements from the literature (Figure 5c in [13]). This final analysis corroborated from a different angle that a tract-target, as derived based on a connectomic approach, may potentially prove useful for unifying the pathophysiological mechanism underlying therapeutic effects of the many stereotactic targets proposed for OCD-DBS.

Given its potential clinical importance, we calculated a final version of the predictive fiber tract using the data from all four cohorts. Anatomical properties of the tract were characterized using additional views in relation to anatomical landmarks for stereotactic planning (Figure 6 and Supplementary Figure 3 in [13]). Anatomically, the tract traverses through the ALIC, connecting the STN and mediodorsal (MD) nucleus of the thalamus with frontal areas including dorsal anterior cingulate cortex (dACC) and ventrolateral prefrontal cortex (vlPFC). We confirmed the anatomical validity of the tract through the expertise of four anatomists as well as discussions with further experts in the field.

The tract identified here was made available in form of an atlas, defined in stereotactic standard (MNI) space, within Lead-DBS software (www.lead-dbs.org). As a first step, such an openly accessible three-dimensional atlas could facilitate retrospective validation or falsification studies. Indeed, since [13] was published, the identified tract has received confirmation via studies from two independent international DBS centers [49,50]. One showed that the tract was predictive of the clinical improvements of ten OCD patients with vALIC/VS DBS [49]. The other study re-calculated the optimal fiber tract for eight patients with VC/VS DBS using the same approach and identified the same fiber bundles [50]. More interestingly, another recent study of 28 Tourette Syndrome patients with GPi DBS showed that modulation of the tract can significantly predict the improvement of OCD symptoms in these patients [51]. In a distant future, and only after multiple additional such replication studies, the published tract atlas may become of value for guiding DBS programming or surgery.

4. Discussion

In this study, data from four cohorts of OCD patients receiving DBS to different target zones were analyzed using a connectomic approach. The same discriminative fiber tract, which connected the STN with dACC and vlPFC, was identified for either the ALIC (Cologne) or the STN (Grenoble) cohort. Based on how well it was connected/activated, this optimal tract target was predictive of good clinical improvement within each cohort. Furthermore, it was also able to significantly predict clinical improvements across DBS cohorts, targets, and centers. Finally, further literature-derived stereotactic stimulation sites proposed for treating OCD appeared to cluster around the tract.

4.1 A unifying tract target for DBS in OCD

First of all, the results of this study integrate with findings put forward by Baldermann et al. 2019 [8], who identified a fiber bundle associated with good clinical response in ALIC-DBS patients. Specifically, the authors elucidated a bundle which connected the thalamus with the medial and lateral PFC and followed a trajectory that passed through the ventral ALIC. Based on the study results, it was concluded that DBS would modulate the fronto-thalamic pathway within the ALIC, which conformed to the assumption that the fronto-striato-thalamic circuit is implicated in OCD [52–54]. Crucially, when extending the analysis by use of two different stimulation targets as done within the scope of the present study, this same tract emerged again and in even more distinct fashion.

The trajectory of the tract identified here largely matches the one of the hyperdirect pathway and originates from prefrontal areas, among which the dACC [55–57]. This prefrontal structure has been discussed to play an important role in the cortico-striato-thalamo-cortical (CSTC) model of OCD pathophysiology [57]. dACC has a wide range of afferent inputs and efferent projections. Aberrant control signal from dysfunctional dACC could be the pathophysiology of OCD symptoms and behaviors [57]. Along similar lines, lesion studies may provide additional evidence toward the prominent role of fiber tracts connecting to this very region. Specifically, direct lesioning of the dACC was consistently reported to improve OCD symptoms in humans [58]. Also, the hyperdirect pathway linking the dACC to the STN was further confirmed (Supplementary Figure 1 and 2 in [13]) when we repeated the same analysis using a synthesized anatomical atlas [55] instead of a normative connectome. It was also supported by a recent study on functional segregation of the ALIC which used a combination of animal and human data [59]. Abnormalities in the

pathway were associated with different psychiatric diseases, including OCD. In other words, the hyperdirect pathway may functionally mediate clinical outcome.

4.2 Toward symptom-specific circuitopathies

However, despite our study provides an initial hint toward a unifying connectomic substrate of DBS effective for reducing global obsessive-compulsive behavior across surgical target sites, our findings also indicated largely different, target-specific connectivity profiles when not weighted by Y-BOCS change scores. Thus, it is conceivable that above and beyond the shared fronto-subcortical tract identified here, each target zone may additionally entertain connections to distinct, target-specific networks, which could potentially exert differential clinical effectiveness on symptoms other than global obsessive-compulsive behavior. Indeed, in a clinical trial in which both the STN and ALIC were directly compared as potential stimulation targets within the same OCD patients, Tyagi et al. [28] showed that STN stimulation preferentially related to improvements in cognitive flexibility while the ALIC target exerted higher impact on mood symptoms.

Importantly, a suchlike concept of symptom-specific effectiveness of stimulation applied to different target zones does not necessarily contradict the main conclusion of the current study, given that in the Tyagi et al. study, both target sites were equally effective in reducing global obsessive-compulsive behavior in addition to their symptom-specific roles. Of note, our analyses were exclusively based on Y-BOCS score improvements, while more granular scores for different symptoms were unavailable for testing the hypothesis of symptom-specific effectiveness. Still, concluding from combined evidence from our findings and those of the Tyagi et al. study, although stimulation to the two targets may in fact modulate the same fiber bundle, this does not necessarily mean that the effects emerging from these two targets are entirely equivalent. Hypothetically, on a patient-by-patient basis, an interventional choice between these two target zones could be based on the prevalent, unique symptom profile an OCD patient may display in addition to global obsessive-compulsive symptomatology. Needless to say, before such a strategy can be safely translated into clinical routine care, the concept must be put under close empirical scrutiny through multiple retrospective replication studies as well as carefully designed prospective trials.

Based on previous studies and our presented results, two testable hypotheses with

implications above and beyond OCD may be proposed. First, different DBS targets may be equally effective in reducing the same symptom. In this line of reasoning, it could be possible that the same tract or therapeutic network was modulated which mediated clinical outcome. Second, different targets may modulate not only one shared network but also other networks that are not shared among targets, which could lead to different effects on other symptoms (for example, as shown in Tyagi et al. 2019 [28]). Therefore, it is conceivable that brain networks modulated by DBS are symptom-specific instead of disease-specific. In other words, by modulating these networks or tracts, specific symptoms involved in a disease would be alleviated, rather than the specific disease. For example, in OCD, different prefrontal sites were found to underly different symptom types [60]. In PD, similar observations were made indicating that primary motor cortex (M1) and supplementary motor area (SMA) were associated with different symptoms [9].

Again, the aim of our study was not to define one most optimal target for OCD-DBS. Instead, we intended to show that multiple proposed targets may exert their therapeutic effectiveness by modulating a shared underlying connectomic substrate. As such, we demonstrated that it is possible predicting symptom-specific clinical outcome across DBS targets using a connectomic based approach. Although the predictive tract in our study was derived based on Y-BOCS improvement, different tracts could have been identified when we repeat the same analysis for other symptoms (depending on data availability).

The concept of symptom-specific networks could potentially ring in an era of increased interventional precision through an enhanced understanding of symptom-specific circuitopathies that will move away more and more from disease-centric strategies. In the future, a broad patient-specific symptom score could potentially be established preoperatively, based on which optimal stimulation targets could be determined as a function of blends of symptom-specific network targets. This framework could lead the way toward precise DBS interventions tailored to each patient's unique symptom profile. We have already started working on this using a fiber-mixing approach, in the hope of establishing a methodology to identify the personalized optimal stimulation target. In this respect, it may also prove useful for overcoming the limitations imposed by a homogeneous interventional strategy applied to heterogeneous patient phenotypes.

4.3 Limitations

There are several limitations to the current work. First, due to the retrospective design,

the results of the study must be interpreted carefully and ideally, prospectively validated.

Second, normative connectome instead of patient-specific dMRI (which is unavailable for most of the patients included) was used to estimate structural connectivity in this study. Such approach could limit the ability of accounting for patient-specific anatomical and connectomic variations. Nevertheless, robustness of models established based on normative connectomes has been shown by means of multiple successful cross-validations across cohorts, and has been further validated and reproduced by groups worldwide [49–51,61]. While the concept of using normative connectomes was introduced in other clinical domains (such as transcranial magnetic stimulation [62]) where patient-specific dMRI data is unavailable, it has also been widely adopted in DBS studies for PD [63] or OCD [64]. Apart from the practical reason that normative connectomes can serve as a suitable alternative in cases where patient-specific data are unavailable, normative data typically also benefits from increased quality of the underlying data and thus displays high signal-to-noise ratio [65–67]. The normative connectome used in this study was derived from 985 subjects released by the HCP project, where images were acquired under state-of-the-art research conditions at an advanced imaging center. Data of comparable quality are usually unavailable in clinical setting. Potentially, a strategy that takes advantage of both normative and individualized dataset should be investigated in the future, to infer from patient-specific connectivity.

Third, nonlinear transformation of electrode localization from patient individual space to the template (MNI) space may result in slight inaccuracies. A scientifically validated, state-of-the-art imaging processing pipeline was used to counteract this limitation as much as possible. A variety of techniques was employed, including brain-shift correction [38], subcortical refinement [38], multispectral normalization with optimal parameters [38,42] and phantom-validated electrode localization [43]. Apart from that, the processing results of each step were meticulously assessed, refined, and corrected by an expert in this area, if necessary.

Fourth, binarized VTAs derived from the finite element method were used for connectivity calculation. However, both estimation of the E-field and the thresholding applied should only be seen as approximations, which are likely unable to truthfully depict every single aspect of the empirical interactions between stimulation current and brain tissues [68,69]. More sophisticated models and methods are currently being developed [69,70] which could prove beneficial for future studies.

Finally, only 50 patients were included in this study. Of these, 33 patients had received post-operative CT, while 17 patients had undergone post-operative MRI, which could be used for electrode localization. Nevertheless, given that numbers of OCD patients treated with DBS are usually small in each respective DBS center world-wide, our analysis was able to pool a relatively large sample when compared to typical studies in this particular indication of DBS. However, going forward, an even larger dataset with homogeneous imaging data would be beneficial to further validate our results. This may especially be the case for attempts of deriving predictors for clinical outcome based on a connectomic approach, which go beyond the correlative nature of the here-presented analysis.

4.4 Conclusions

In summary, in this study, we showed that despite differences in the overall connectivity patterns of electrodes between STN- and ALIC DBS cohorts treated for OCD, a common fiber tract shared across stimulation targets and centers emerged when connectivity was weighted by clinical outcome. The identified tract target demonstrated high predictive robustness in cross-predictions, and integrated published reports and off-site replications. The same approach applied in this study could potentially be used to define connectomic targets for DBS in other diseases which may harmonize respectively proposed stimulation sites.

References

1. Lozano, A. M., & Lipsman, N. (2013). Probing and Regulating Dysfunctional Circuits Using Deep Brain Stimulation. *Neuron*, *77*(3), 406–424. https://doi.org/10.1016/j.neuron.2013.01.020

2. Horn, A., Reich, M., Vorwerk, J., Li, N., Wenzel, G., Fang, Q., Schmitz-Hübsch, T., Nickl, R., Kupsch, A., Volkmann, J., Kühn, A. A., & Fox, M. D. (2017). Connectivity Predicts deep brain stimulation outcome in Parkinson disease. *Annals of Neurology*, *82*(1), 67–78. https://doi.org/10.1002/ana.24974

3. Horn, A. (2019). The impact of modern-day neuroimaging on the field of deep brain stimulation. *Current Opinion in Neurology*, *Publish Ahead of Print*. https://doi.org/10.1097/WCO.0000000000000679

4. Schaerer, J., Roche, F., & Belaroussi, B. (2014). A generic interpolator for multi-label images. *The Insight Journal*, 950.

5. Liebrand, L. C., Caan, M. W. A., Schuurman, P. R., van den Munckhof, P., Figee, M., Denys, D., & van Wingen, G. A. (2019). Individual white matter bundle trajectories are associated with deep brain stimulation response in obsessive-compulsive disorder. *Brain Stimulation*, *12*(2), 353–360. https://doi.org/10.1016/j.brs.2018.11.014

6. Heilbronner, S. R., Safadi, Z., & Haber, S. N. (2016). Neurocircuits commonly involved in psychiatric disorders and their stimulation and lesion therapies. In *Neuromodulation in Psychiatry* (pp. 27–48). John Wiley & Sons, Ltd. https://doi.org/10.1002/9781118801086.ch3

7. Sporns, O., Tononi, G., & Kötter, R. (2005). The Human Connectome: A Structural Description of the Human Brain. *PLOS Computational Biology*, *1*(4), e42. https://doi.org/10.1371/journal.pcbi.0010042

8. Baldermann, J. C., Melzer, C., Zapf, A., Kohl, S., Timmermann, L., Tittgemeyer, M., Huys, D., Visser-Vandewalle, V., Kühn, A. A., Horn, A., & Kuhn, J. (2019). Connectivity profile predictive of effective deep brain stimulation in obsessive compulsive disorder. *Biological Psychiatry*. https://doi.org/10.1016/j.biopsych.2018.12.019

9. Akram, H., Sotiropoulos, S. N., Jbabdi, S., Georgiev, D., Mahlknecht, P., Hyam, J., Foltynie, T., Limousin, P., De Vita, E., Jahanshahi, M., Hariz, M., Ashburner, J., Behrens, T., & Zrinzo, L. (2017). Subthalamic deep brain stimulation sweet spots and hyperdirect cortical connectivity in Parkinson's disease. *NeuroImage*, *158*, 332–345. https://doi.org/10.1016/j.neuroimage.2017.07.012

10. Middlebrooks, E. H., Tuna, I. S., Grewal, S. S., Almeida, L., Heckman, M. G., Lesser, E. R., Foote, K. D., Okun, M. S., & Holanda, V. M. (2018). Segmentation of the Globus Pallidus Internus Using Probabilistic Diffusion Tractography for Deep Brain Stimulation Targeting in Parkinson Disease. *American Journal of Neuroradiology*, *39*(6), 1127–1134. https://doi.org/10.3174/ajnr.A5641

11. Vanegas-Arroyave, N., Lauro, P. M., Huang, L., Hallett, M., Horovitz, S. G., Zaghloul, K. A., & Lungu, C. (2016). Tractography patterns of subthalamic nucleus deep brain stimulation. *Brain*, *139*(4), 1200–1210. https://doi.org/10.1093/brain/aww020

12. Henderson, J. M. M. D. (2012). "Connectomic surgery": Diffusion tensor imaging (DTI) tractography as a targeting modality for surgical modulation of neural networks. *Frontiers in Integrative Neuroscience*, *6*. https://doi.org/10.3389/fnint.2012.00015

13. Li, N., Baldermann, J. C., Kibleur, A., Treu, S., Akram, H., Elias, G. J. B., Boutet, A., Lozano, A. M., Al-Fatly, B., Strange, B., Barcia, J. A., Zrinzo, L., Joyce, E.,

Chabardes, S., Visser-Vandewalle, V., Polosan, M., Kuhn, J., Kühn, A. A., & Horn, A. (2020). A unified connectomic target for deep brain stimulation in obsessive-compulsive disorder. *Nature Communications*, *11*(1), 3364. https://doi.org/10.1038/s41467-020-16734-3

14. Ruscio, A. M., Stein, D. J., Chiu, W. T., & Kessler, R. C. (2010). The epidemiology of obsessive-compulsive disorder in the National Comorbidity Survey Replication. *Molecular Psychiatry*, *15*(1), 53–63. https://doi.org/10.1038/mp.2008.94
15. Mallet, L., Mesnage, V., Houeto, J.-L., Pelissolo, A., Yelnik, J., Behar, C., Gargiulo, M., Welter, M.-L., Bonnet, A.-M., Pillon, B., Cornu, P., Dormont, D., Pidoux, B., Allilaire, J.-F., & Agid, Y. (2002). Compulsions, Parkinson's disease, and stimulation. *The Lancet*, *360*(9342), 1302–1304. https://doi.org/10.1016/S0140-6736(02)11339-0
16. Chabardès, S., Polosan, M., Krack, P., Bastin, J., Krainik, A., David, O., Bougerol, T., & Benabid, A. L. (2013). Deep Brain Stimulation for Obsessive-Compulsive Disorder: Subthalamic Nucleus Target. *World Neurosurgery*, *80*(3), S31.e1-S31.e8. https://doi.org/10.1016/j.wneu.2012.03.010
17. Sturm, V., Lenartz, D., Koulousakis, A., Treuer, H., Herholz, K., Klein, J. C., & Klosterkötter, J. (2003). The nucleus accumbens: A target for deep brain stimulation in obsessive–compulsive- and anxiety-disorders. *Journal of Chemical Neuroanatomy*, *26*(4), 293–299. https://doi.org/10.1016/j.jchemneu.2003.09.003
18. Aouizerate, B., Cuny, E., Martin-Guehl, C., Guehl, D., Amieva, H., Benazzouz, A., Fabrigoule, C., Allard, M., Rougier, A., Bioulac, B., Tignol, J., & Burbaud, P. (2004). Deep brain stimulation of the ventral caudate nucleus in the treatment of obsessive—compulsive disorder and major depression: Case report. *Journal of Neurosurgery*, *101*(4), 682–686. https://doi.org/10.3171/jns.2004.101.4.0682

19. Franzini, A., Messina, G., Gambini, O., Muffatti, R., Scarone, S., Cordella, R., & Broggi, G. (2010). Deep-brain stimulation of the nucleus accumbens in obsessive compulsive disorder: Clinical, surgical and electrophysiological considerations in two consecutive patients. *Neurological Sciences*, *31*(3), 353–359. https://doi.org/10.1007/s10072-009-0214-8

20. Greenberg, B. D., Malone, D. A., Friehs, G. M., Rezai, A. R., Kubu, C. S., Malloy, P. F., Salloway, S. P., Okun, M. S., Goodman, W. K., & Rasmussen, S. A. (2006). Three-Year Outcomes in Deep Brain Stimulation for Highly Resistant Obsessive–Compulsive Disorder. *Neuropsychopharmacology*, *31*(11), 2384–2393. https://doi.org/10.1038/sj.npp.1301165

21. Jiménez-Ponce, F., Velasco-Campos, F., Castro-Farfán, G., Nicolini, H., Velasco, A. L., Salín-Pascual, R., Trejo, D., & Criales, J. L. (2009). Preliminary Study in Patients With Obsessive-Compulsive Disorder Treated With Electrical Stimulation in the Inferior Thalamic Peduncle. *Operative Neurosurgery*, *65*(suppl_6), ons203–ons209. https://doi.org/10.1227/01.NEU.0000345938.39199.90

22. Lee, D. J., Dallapiazza, R. F., De Vloo, P., Elias, G. J. B., Fomenko, A., Boutet, A., Giacobbe, P., & Lozano, A. M. (2019). Inferior thalamic peduncle deep brain stimulation for treatment-refractory obsessive-compulsive disorder: A phase 1 pilot trial. *Brain Stimulation*, *12*(2), 344–352. https://doi.org/10.1016/j.brs.2018.11.012

23. Luyten, L., Hendrickx, S., Raymaekers, S., Gabriëls, L., & Nuttin, B. (2016). Electrical stimulation in the bed nucleus of the stria terminalis alleviates severe obsessive-compulsive disorder. *Molecular Psychiatry*, *21*(9), 1272–1280. https://doi.org/10.1038/mp.2015.124

24. Nair, G., Evans, A., Bear, R. E., Velakoulis, D., & Bittar, R. G. (2014). The

anteromedial GPi as a new target for deep brain stimulation in obsessive compulsive disorder. *Journal of Clinical Neuroscience*, *21*(5), 815–821. https://doi.org/10.1016/j.jocn.2013.10.003

25. Coenen, V. A., Schlaepfer, T. E., Goll, P., Reinacher, P. C., Voderholzer, U., Elst, L. T. van, Urbach, H., & Freyer, T. (2017). The medial forebrain bundle as a target for deep brain stimulation for obsessive-compulsive disorder. *CNS Spectrums*, *22*(3), 282–289. https://doi.org/10.1017/S1092852916000286
26. Maarouf, M., Neudorfer, C., Majdoub, F. E., Lenartz, D., Kuhn, J., & Sturm, V. (2016). Deep Brain Stimulation of Medial Dorsal and Ventral Anterior Nucleus of the Thalamus in OCD: A Retrospective Case Series. *PLOS ONE*, *11*(8), e0160750. https://doi.org/10.1371/journal.pone.0160750
27. Borders, C., Hsu, F., Sweidan, A. J., Matei, E. S., & Bota, R. G. (2018). Deep brain stimulation for obsessive compulsive disorder: A review of results by anatomical target. *Mental Illness*, *10*(2). https://doi.org/10.4081/mi.2018.7900
28. Tyagi, H., Apergis-Schoute, A. M., Akram, H., Foltynie, T., Limousin, P., Drummond, L. M., Fineberg, N. A., Matthews, K., Jahanshahi, M., Robbins, T. W., Sahakian, B. J., Zrinzo, L., Hariz, M., & Joyce, E. M. (2019). A Randomized Trial Directly Comparing Ventral Capsule and Anteromedial Subthalamic Nucleus Stimulation in Obsessive-Compulsive Disorder: Clinical and Imaging Evidence for Dissociable Effects. *Biological Psychiatry*. https://doi.org/10.1016/j.biopsych.2019.01.017
29. Deuschl, G., Schade-Brittinger, C., Krack, P., Volkmann, J., Schäfer, H., Bötzel, K., Daniels, C., Deutschländer, A., Dillmann, U., Eisner, W., Gruber, D., Hamel, W., Herzog, J., Hilker, R., Klebe, S., Kloß, M., Koy, J., Krause, M., Kupsch, A., … Voges, J. (2006). A Randomized Trial of Deep-Brain Stimulation for Parkinson's

Disease. *New England Journal of Medicine*, *355*(9), 896–908. https://doi.org/10.1056/NEJMoa060281

30. Ostrem, J. L., Racine, C. A., Glass, G. A., Grace, J. K., Volz, M. M., Heath, S. L., & Starr, P. A. (2011). Subthalamic nucleus deep brain stimulation in primary cervical dystonia. *Neurology*, *76*(10), 870–878. https://doi.org/10.1212/WNL.0b013e31820f2e4f
31. Vissani, M., Cordella, R., Micera, S., Romito, L. M., & Mazzoni, A. (2019). Spatio-temporal structure of single neuron subthalamic activity in Tourette Syndrome explored during DBS procedures. *BioRxiv*, 532200. https://doi.org/10.1101/532200
32. Polosan, M., Droux, F., Kibleur, A., Chabardes, S., Bougerol, T., David, O., Krack, P., & Voon, V. (2019). Affective modulation of the associative-limbic subthalamic nucleus: Deep brain stimulation in obsessive–compulsive disorder. *Translational Psychiatry*, *9*(1), 73. https://doi.org/10.1038/s41398-019-0404-y
33. Alkemade, A., Groot, J. M., & Forstmann, B. U. (2018). Do We Need a Human post mortem Whole-Brain Anatomical Ground Truth in in vivo Magnetic Resonance Imaging? *Frontiers in Neuroanatomy*, *12*. https://doi.org/10.3389/fnana.2018.00110
34. Li, N., Baldermann, J. C., Kibleur, A., Treu, S., Elias, G. J. B., Boutet, A., Lozano, A. M., Chabardes, S., Visser-Vandewalle, V., Polosan, M., Kuhn, J., Kühn, A. A., & Horn, A. (2019). Toward a unified connectomic target for deep brain stimulation in obsessive-compulsive disorder. *BioRxiv*, 608786. https://doi.org/10.1101/608786
35. Huys, D., Kohl, S., Baldermann, J. C., Timmermann, L., Sturm, V., Visser-Vandewalle, V., & Kuhn, J. (2019). Open-label trial of anterior limb of internal capsule–nucleus accumbens deep brain stimulation for obsessive-compulsive

disorder: Insights gained. *Journal of Neurology, Neurosurgery & Psychiatry*, jnnp-2018-318996. https://doi.org/10.1136/jnnp-2018-318996

36. Barcia, J. A., Avecillas-Chasín, J. M., Nombela, C., Arza, R., García-Albea, J., Pineda-Pardo, J. A., Reneses, B., & Strange, B. A. (2018). Personalized striatal targets for deep brain stimulation in obsessive-compulsive disorder. *Brain Stimulation*. https://doi.org/10.1016/j.brs.2018.12.226
37. Horn, A., & Kühn, A. A. (2015). Lead-DBS: A toolbox for deep brain stimulation electrode localizations and visualizations. *NeuroImage*, *107*, 127–135. https://doi.org/10.1016/j.neuroimage.2014.12.002
38. Horn, A., Li, N., Dembek, T. A., Kappel, A., Boulay, C., Ewert, S., Tietze, A., Husch, A., Perera, T., Neumann, W.-J., Reisert, M., Si, H., Oostenveld, R., Rorden, C., Yeh, F.-C., Fang, Q., Herrington, T. M., Vorwerk, J., & Kühn, A. A. (2019). Lead-DBS v2: Towards a comprehensive pipeline for deep brain stimulation imaging. *NeuroImage*, *184*, 293–316. https://doi.org/10.1016/j.neuroimage.2018.08.068
39. Avants, B. B., Tustison, N., & Song, G. (2009). Advanced normalization tools (ANTS). *Insight j*, *2*, 1–35.
40. Fonov, V., Evans, A., McKinstry, R., Almli, C., & Collins, D. (2009). Unbiased nonlinear average age-appropriate brain templates from birth to adulthood. *NeuroImage*, *47*, S102. https://doi.org/10.1016/S1053-8119(09)70884-5
41. Avants, B. B., Epstein, C. L., Grossman, M., & Gee, J. C. (2008). Symmetric Diffeomorphic Image Registration with Cross-Correlation: Evaluating Automated Labeling of Elderly and Neurodegenerative Brain. *Medical Image Analysis*, *12*(1), 26–41. https://doi.org/10.1016/j.media.2007.06.004
42. Ewert, S., Horn, A., Finkel, F., Li, N., Kühn, A. A., & Herrington, T. M. (2019). Optimization and comparative evaluation of nonlinear deformation algorithms for

atlas-based segmentation of DBS target nuclei. *NeuroImage*, *184*, 586–598. https://doi.org/10.1016/j.neuroimage.2018.09.061

43. Husch, A., V. Petersen, M., Gemmar, P., Goncalves, J., & Hertel, F. (2017). PaCER - A fully automated method for electrode trajectory and contact reconstruction in deep brain stimulation. *NeuroImage : Clinical*, *17*, 80–89. https://doi.org/10.1016/j.nicl.2017.10.004
44. Vorwerk, J., Oostenveld, R., Piastra, M. C., Magyari, L., & Wolters, C. H. (2018). The FieldTrip-SimBio pipeline for EEG forward solutions. *BioMedical Engineering OnLine*, *17*(1), 37. https://doi.org/10.1186/s12938-018-0463-y
45. Glasser, M. F., Smith, S. M., Marcus, D. S., Andersson, J. L. R., Auerbach, E. J., Behrens, T. E. J., Coalson, T. S., Harms, M. P., Jenkinson, M., Moeller, S., Robinson, E. C., Sotiropoulos, S. N., Xu, J., Yacoub, E., Ugurbil, K., & Van Essen, D. C. (2016). The Human Connectome Project's neuroimaging approach. *Nature Neuroscience*, *19*(9), 1175–1187. https://doi.org/10.1038/nn.4361
46. Ewert, S., Plettig, P., Li, N., Chakravarty, M. M., Collins, D. L., Herrington, T. M., Kühn, A. A., & Horn, A. (2018). Toward defining deep brain stimulation targets in MNI space: A subcortical atlas based on multimodal MRI, histology and structural connectivity. *NeuroImage*, *170*, 271–282. https://doi.org/10.1016/j.neuroimage.2017.05.015
47. Horn, A., Kühn, A. A., Merkl, A., Shih, L., Alterman, R., & Fox, M. (2017). Probabilistic conversion of neurosurgical DBS electrode coordinates into MNI space. *NeuroImage*, *150*, 395–404. https://doi.org/10.1016/j.neuroimage.2017.02.004
48. Neumann, W.-J., Schroll, H., Marcelino, de A., Luisa, A., Horn, A., Ewert, S., Irmen, F., Krause, P., Schneider, G.-H., Hamker, F., & Kühn, A. A. (2018).

Functional segregation of basal ganglia pathways in Parkinson's disease. *Brain*, *141*(9), 2655–2669. https://doi.org/10.1093/brain/awy206

49. Smith, A. H., Choi, K. S., Waters, A. C., Aloysi, A., Mayberg, H. S., Kopell, B. H., & Figee, M. (2021). Replicable effects of deep brain stimulation for obsessive-compulsive disorder. *Brain Stimulation*, *14*(1), 1–3. https://doi.org/10.1016/j.brs.2020.10.016
50. Vlis, T. A. M. B. van der, Ackermans, L., Mulders, A. E. P., Vrij, C. A., Schruers, K., Temel, Y., Duits, A., & Leentjens, A. F. G. (2020). Ventral Capsule/Ventral Striatum Stimulation in Obsessive-Compulsive Disorder: Toward a Unified Connectomic Target for Deep Brain Stimulation? *Neuromodulation: Technology at the Neural Interface*, *n/a*(n/a). https://doi.org/10.1111/ner.13339
51. Johnson, K. A., Duffley, G., Foltynie, T., Hariz, M., Zrinzo, L., Joyce, E. M., Akram, H., Servello, D., Galbiati, T. F., Bona, A., Porta, M., Meng, F.-G., Leentjens, A. F. G., Gunduz, A., Hu, W., Foote, K. D., Okun, M. S., & Butson, C. R. (2020). Basal Ganglia Pathways Associated with Therapeutic Pallidal Deep Brain Stimulation for Tourette Syndrome. *Biological Psychiatry: Cognitive Neuroscience and Neuroimaging*. https://doi.org/10.1016/j.bpsc.2020.11.005
52. Bourne, S. K., Eckhardt, C. A., Sheth, S. A., & Eskandar, E. N. (2012). Mechanisms of deep brain stimulation for obsessive compulsive disorder: Effects upon cells and circuits. *Frontiers in Integrative Neuroscience*, *6*. https://doi.org/10.3389/fnint.2012.00029
53. Figee, M., Luigjes, J., Smolders, R., Valencia-Alfonso, C.-E., van Wingen, G., de Kwaasteniet, B., Mantione, M., Ooms, P., de Koning, P., Vulink, N., Levar, N., Droge, L., van den Munckhof, P., Schuurman, P. R., Nederveen, A., van den Brink, W., Mazaheri, A., Vink, M., & Denys, D. (2013). Deep brain stimulation

restores frontostriatal network activity in obsessive-compulsive disorder. *Nature Neuroscience*, *16*(4), 386–387. https://doi.org/10.1038/nn.3344

54. Dunlop, K., Woodside, B., Olmsted, M., Colton, P., Giacobbe, P., & Downar, J. (2016). Reductions in Cortico-Striatal Hyperconnectivity Accompany Successful Treatment of Obsessive-Compulsive Disorder with Dorsomedial Prefrontal rTMS. *Neuropsychopharmacology*, *41*(5), 1395–1403. https://doi.org/10.1038/npp.2015.292

55. Petersen, M. V., Mlakar, J., Haber, S. N., Parent, M., Smith, Y., Strick, P. L., Griswold, M. A., & McIntyre, C. C. (2019). Holographic Reconstruction of Axonal Pathways in the Human Brain. *Neuron*, *104*(6), 1056-1064.e3. https://doi.org/10.1016/j.neuron.2019.09.030

56. Haynes, W. I. A., & Haber, S. N. (2013). The Organization of Prefrontal-Subthalamic Inputs in Primates Provides an Anatomical Substrate for Both Functional Specificity and Integration: Implications for Basal Ganglia Models and Deep Brain Stimulation. *Journal of Neuroscience*, *33*(11), 4804–4814. https://doi.org/10.1523/JNEUROSCI.4674-12.2013

57. McGovern, R. A., & Sheth, S. A. (2017). Role of the dorsal anterior cingulate cortex in obsessive-compulsive disorder: Converging evidence from cognitive neuroscience and psychiatric neurosurgery. *Journal of Neurosurgery*, *126*(1), 132–147. https://doi.org/10.3171/2016.1.JNS15601

58. Dougherty, D. D., Baer, L., Cosgrove, G. R., Cassem, E. H., Price, B. H., Nierenberg, A. A., Jenike, M. A., & Rauch, S. L. (2002). Prospective Long-Term Follow-Up of 44 Patients Who Received Cingulotomy for Treatment-Refractory Obsessive-Compulsive Disorder. *American Journal of Psychiatry*, *159*(2), 269–275. https://doi.org/10.1176/appi.ajp.159.2.269

59. Safadi, Z., Grisot, G., Jbabdi, S., Behrens, T. E., Heilbronner, S. R., McLaughlin, N. C. R., Mandeville, J., Versace, A., Phillips, M. L., Lehman, J. F., Yendiki, A., & Haber, S. N. (2018). Functional Segmentation of the Anterior Limb of the Internal Capsule: Linking White Matter Abnormalities to Specific Connections. *Journal of Neuroscience*, *38*(8), 2106–2117. https://doi.org/10.1523/JNEUROSCI.2335-17.2017

60. Mataix-Cols, D., Wooderson, S., Lawrence, N., Brammer, M. J., Speckens, A., & Phillips, M. L. (2004). Distinct Neural Correlates of Washing, Checking, and Hoarding SymptomDimensions in Obsessive-compulsive Disorder. *Archives of General Psychiatry*, *61*(6), 564–576. https://doi.org/10.1001/archpsyc.61.6.564

61. Mosley, P. E., Windels, F., Morris, J., Coyne, T., Marsh, R., Giorni, A., Mohan, A., Sachdev, P., O'Leary, E., Boschen, M., Sah, P., & Silburn, P. A. (2021). A randomised, double-blind, sham-controlled trial of deep brain stimulation of the bed nucleus of the stria terminalis for treatment-resistant obsessive-compulsive disorder. *Translational Psychiatry*, *11*(1), 1–17. https://doi.org/10.1038/s41398-021-01307-9

62. Weigand, A., Horn, A., Caballero, R., Cooke, D., Stern, A. P., Taylor, S. F., Press, D., Pascual-Leone, A., & Fox, M. D. (2018). Prospective Validation That Subgenual Connectivity Predicts Antidepressant Efficacy of Transcranial Magnetic Stimulation Sites. *Biological Psychiatry*, *84*(1), 28–37. https://doi.org/10.1016/j.biopsych.2017.10.028

63. Wang, Q., Akram, H., Muthuraman, M., Gonzalez-Escamilla, G., Sheth, S. A., Oxenford, S., Yeh, F.-C., Groppa, S., Vanegas-Arroyave, N., Zrinzo, L., Li, N., Kühn, A., & Horn, A. (2021). Normative vs. Patient-specific brain connectivity in deep brain stimulation. *NeuroImage*, *224*, 117307.

https://doi.org/10.1016/j.neuroimage.2020.117307

64. Baldermann, J. C., Melzer, C., Zapf, A., Kohl, S., Timmermann, L., Tittgemeyer, M., Huys, D., Visser-Vandewalle, V., Kühn, A. A., Horn, A., & Kuhn, J. (2019). Connectivity Profile Predictive of Effective Deep Brain Stimulation in Obsessive-Compulsive Disorder. *Biological Psychiatry*, *85*(9), 735–743. https://doi.org/10.1016/j.biopsych.2018.12.019

65. Horn, A., & Fox, M. D. (2020). Opportunities of Connectomic Neuromodulation. *NeuroImage*, 117180. https://doi.org/10.1016/j.neuroimage.2020.117180

66. Greene, D. J., Marek, S., Gordon, E. M., Siegel, J. S., Gratton, C., Laumann, T. O., Gilmore, A. W., Berg, J. J., Nguyen, A. L., Dierker, D., Van, A. N., Ortega, M., Newbold, D. J., Hampton, J. M., Nielsen, A. N., McDermott, K. B., Roland, J. L., Norris, S. A., Nelson, S. M., … Dosenbach, N. U. F. (2020). Integrative and Network-Specific Connectivity of the Basal Ganglia and Thalamus Defined in Individuals. *Neuron*, *105*(4), 742-758.e6. https://doi.org/10.1016/j.neuron.2019.11.012

67. Jakab, A., Werner, B., Piccirelli, M., Kovács, K., Martin, E., Thornton, J. S., Yousry, T., Szekely, G., & O'Gorman Tuura, R. (2016). Feasibility of Diffusion Tractography for the Reconstruction of Intra-Thalamic and Cerebello-Thalamic Targets for Functional Neurosurgery: A Multi-Vendor Pilot Study in Four Subjects. *Frontiers in Neuroanatomy*, *10*. https://doi.org/10.3389/fnana.2016.00076

68. Duffley, G., Anderson, D. N., Vorwerk, J., Dorval, A. D., & Butson, C. R. (2019). Evaluation of methodologies for computing the deep brain stimulation volume of tissue activated. *Journal of Neural Engineering*, *16*(6), 066024. https://doi.org/10.1088/1741-2552/ab3c95

69. Gunalan, K., Chaturvedi, A., Howell, B., Duchin, Y., Lempka, S. F., Patriat, R.,

Sapiro, G., Harel, N., & McIntyre, C. C. (2017). Creating and parameterizing patient-specific deep brain stimulation pathway-activation models using the hyperdirect pathway as an example. *PLOS ONE*, *12*(4), e0176132. https://doi.org/10.1371/journal.pone.0176132

70. Butenko, K., Bahls, C., Schröder, M., Köhling, R., & Rienen, U. van. (2020). OSS-DBS: Open-source simulation platform for deep brain stimulation with a comprehensive automated modeling. *PLOS Computational Biology*, *16*(7), e1008023. https://doi.org/10.1371/journal.pcbi.1008023

Statutory Declaration

“I, **Ningfei Li**, by personally signing this document in lieu of an oath, hereby affirm that I prepared the submitted dissertation on the topic **Connectomic Targets for Deep Brain Stimulation (Connectomic Targets für die Tiefenhirnstimulation)**, independently and without the support of third parties, and that I used no other sources and aids than those stated.

All parts which are based on the publications or presentations of other authors, either in letter or in spirit, are specified as such in accordance with the citing guidelines. The sections on methodology (in particular regarding practical work, laboratory regulations, statistical processing) and results (in particular regarding figures, charts and tables) are exclusively my responsibility.

Furthermore, I declare that I have correctly marked all of the data, the analyses, and the conclusions generated from data obtained in collaboration with other persons, and that I have correctly marked my own contribution and the contributions of other persons (cf. declaration of contribution). I have correctly marked all texts or parts of texts that were generated in collaboration with other persons.

My contributions to any publications to this dissertation correspond to those stated in the below joint declaration made together with the supervisor. All publications created within the scope of the dissertation comply with the guidelines of the ICMJE (International Committee of Medical Journal Editors; www.icmje.org) on authorship. In addition, I declare that I shall comply with the regulations of Charité – Universitätsmedizin Berlin on ensuring good scientific practice.

I declare that I have not yet submitted this dissertation in identical or similar form to another Faculty.

The significance of this statutory declaration and the consequences of a false statutory declaration under criminal law (Sections 156, 161 of the German Criminal Code) are known to me.”

Date Signature

Declaration of your own contribution to the publication

Ningfei Li contributed the following to the below listed publication:

Publication 1: **Li, N.**, Baldermann, J.C., Kibleur, A., Treu, S., Akram, H., Elias, G.J.B., Boutet, A., Lozano, A.M., Al-Fatly, B., Strange, B., Barcia, J.A., Zrinzo, L., Joyce, E., Chabardes, S., Visser-Vandewalle, V., Polosan, M., Kuhn, J., Kühn, A.A., Horn, A.. **A unified connectomic target for deep brain stimulation in obsessivecompulsive disorder**. **Nature Communications**, **2020**.

Contribution (please set out in detail):
I conceptualized the study together with my supervisor Dr. Andreas Horn. I am one of the core developers of the software (LeadDBS) used for data analysis. I conducted all the analysis, including MRI/CT image pre-processing, electrode localization for the patient cohorts from Grenoble and London, volume of tissue activated estimation, connectivity analysis and statistical analysis. I created Table 1 and Table 2 in the paper. I created figure 1-5 in the paper. I wrote the draft of the manuscript. I created figure 1-3 in the supplementary material.

_____
Signature, date and stamp of first supervising university professor / lecturer

_____
Signature of doctoral candidate

Extract from the Journal Summary List

Journal Data Filtered By: **Selected JCR Year: 2017** Selected Editions: SCIE,SSCI
Selected Categories: **"MULTIDISCIPLINARY SCIENCES"** Selected Category Scheme: WoS

Gesamtanzahl: 64 Journale

Rank	Full Journal Title	Total Cites	Journal Impact Factor	Eigenfactor Score
1	NATURE	710,766	41.577	1.355810
2	SCIENCE	645,132	41.058	1.127160
3	Nature Communications	178,348	12.353	0.926560
4	Science Advances	10,194	11.511	0.057080
5	PROCEEDINGS OF THE NATIONAL ACADEMY OF SCIENCES OF THE UNITED STATES OF AMERICA	637,268	9.504	1.108220
6	National Science Review	952	9.408	0.004340
7	GigaScience	1,694	7.267	0.011030
8	Scientific Data	1,567	5.305	0.008550
9	Journal of Advanced Research	1,843	4.327	0.003820
10	Annals of the New York Academy of Sciences	46,160	4.277	0.033270
11	Science Bulletin	1,952	4.136	0.005900
12	Scientific Reports	192,841	4.122	0.718960
13	Journal of the Royal Society Interface	11,357	3.355	0.030960
14	Research Synthesis Methods	1,374	3.218	0.006030
15	PLoS One	582,877	2.766	1.862350
16	PHILOSOPHICAL TRANSACTIONS OF THE ROYAL SOCIETY A-MATHEMATICAL PHYSICAL AND ENGINEERING SCIENCES	17,807	2.746	0.028220
17	Royal Society Open Science	2,145	2.504	0.009260
18	PROCEEDINGS OF THE ROYAL SOCIETY A-MATHEMATICAL PHYSICAL AND ENGINEERING SCIENCES	17,157	2.410	0.018270
19	PeerJ	7,377	2.118	0.031600
20	NPJ Microgravity	94	2.000	0.000350
21	SCIENCE AND ENGINEERING ETHICS	1,496	1.859	0.002520
22	COMPLEXITY	1,369	1.829	0.002380
23	Science of Nature	324	1.789	0.001260

Publication

nature COMMUNICATIONS

ARTICLE

https://doi.org/10.1038/s41467-020-16734-3 OPEN

A unified connectomic target for deep brain stimulation in obsessive-compulsive disorder

Ningfei Li[1✉], Juan Carlos Baldermann[2], Astrid Kibleur[3,4], Svenja Treu[5], Harith Akram[6,7], Gavin J. B. Elias[8], Alexandre Boutet[8,9], Andres M. Lozano[8], Bassam Al-Fatly[1], Bryan Strange[5], Juan A. Barcia[10], Ludvic Zrinzo[6,7], Eileen Joyce[6,7], Stephan Chabardes[3], Veerle Visser-Vandewalle[11], Mircea Polosan[3,12,13], Jens Kuhn[2,14], Andrea A. Kühn[1] & Andreas Horn[1]

Multiple surgical targets for treating obsessive-compulsive disorder with deep brain stimulation (DBS) have been proposed. However, different targets may modulate the same neural network responsible for clinical improvement. We analyzed data from four cohorts of patients ($N = 50$) that underwent DBS to the anterior limb of the internal capsule (ALIC), the nucleus accumbens or the subthalamic nucleus (STN). The same fiber bundle was associated with optimal clinical response in cohorts targeting either structure. This bundle connected frontal regions to the STN. When informing the tract target based on the first cohort, clinical improvements in the second could be significantly predicted, and vice versa. To further confirm results, clinical improvements in eight patients from a third center and six patients from a fourth center were significantly predicted based on their stimulation overlap with this tract. Our results show that connectivity-derived models may inform clinical improvements across DBS targets, surgeons and centers. The identified tract target is openly available in atlas form.

[1] Charité – Universitätsmedizin Berlin, corporate member of Freie Universität Berlin, Humboldt-Universität zu Berlin, and Berlin Institute of Health, Movement Disorders and Neuromodulation Unit, Department for Neurology, Charitéplatz 1, 10117 Berlin, Germany. [2] Department of Psychiatry and Psychotherapy, Department of Neurology, University of Cologne, Medical Faculty, Cologne, Germany. [3] Univ. Grenoble Alpes, 38000 Grenoble, France. [4] OpenMind Innovation, 75008 Paris, France. [5] Laboratory for Clinical Neuroscience, Centre for Biomedical Technology, Universidad Politecnica de Madrid, Madrid, Spain. [6] Department of Clinical and Movement Neurosciences, UCL Queen Square Institute of Neurology, London, UK. [7] National Hospital for Neurology and Neurosurgery, UCL Queen Square Institute of Neurology, London, UK. [8] University Health Network, Toronto, ON, Canada. [9] Joint Department of Medical Imaging, University of Toronto, Toronto, ON, Canada. [10] Hospital Clínico San Carlos, Neurosurgery Department, Universidad Complutense de Madrid, Madrid, Spain. [11] Department of Stereotactic and Functional Neurosurgery, University of Cologne, Cologne, Germany. [12] Inserm, U1216, Grenoble Institut des Neurosciences, 38000 Grenoble, France. [13] Psychiatry Department, CHU Grenoble Alpes, 38000 Grenoble, France. [14] Department of Psychiatry, Psychotherapy and Psychosomatics, EVKLN, Johanniter Hospital Oberhausen, Oberhausen, Germany. ✉email: ningfei.li@charite.de

Obsessive-compulsive disorder (OCD) is a debilitating disease with a life-time prevalence of around 2.3%[1]. Treatment of severe cases by deep brain stimulation (DBS) to the ALIC has been approved by the FDA (Humanitarian Device Exemption) in 2009[2]. A variety of other targets have been proposed, however, including the STN[3,4], nucleus accumbens (NAcc)[5], ventral capsule/ventral striatum (VC/VS)[6], inferior thalamic peduncle (ITP)[7], bed nucleus of the stria terminalis (BNST)[8], anteromedial globus pallidus interna (amGPi)[9], superolateral branch of the medial forebrain bundle (slMFB)[10] and medial dorsal and ventral anterior nuclei of the thalamus (MD/vANT)[11] (for an overview see ref. [12]). A recent prospective clinical trial implanted four electrodes per patient with one pair in the STN and one in the ALIC[13].

In parallel, DBS has experienced a conceptual paradigm-shift away from focal stimulation of specific brain nuclei (such as the subthalamic nucleus or globus pallidus in Parkinson's disease; PD) toward modulating distributed brain networks (such as the motor basal-ganglia cortical cerebellar loop in PD)[10,14–17]. Although the concept of modulating white-matter tracts (instead of gray matter nuclei) is certainly not new (and anterior capsulotomy was introduced in the ~1950s by Talairach and Leksell[18]), novel MRI technologies such as diffusion-weighted imaging-based tractography are now increasingly used in functional neurosurgery in order to more deliberately target white-matter tracts[16]. In this translational development, the Coenen and Mayberg groups should be explicitly mentioned, among others, for pioneering and rapidly translating the use of tractography to functional surgery since around 2009[10,14,15,19].

It could be possible that, of the multiple targets proposed, some —or most—may in fact modulate the same brain network to alleviate symptoms. Such a concept has been proposed in the past by Schlaepfer and colleagues for the case of treatment-refractory depression[20]. Namely, the superolateral branch of the medial forebrain bundle may connect most if not all surgical targets that were proposed for treatment of depression (e.g. subgenual cortex, ALIC, NAcc, habenula). Thus, in theory, the tract itself could be a surgical target—and could be modulated in a similar way when targeting various points along its anatomical course. Accordingly, already, Coenen et al.[10] surgically implanted electrodes to directly target this tract instead of a localized target, also in OCD. The tract connected the ventral tegmental area and the prefrontal cortex and authors referred to it as the superolateral branch of the medial forebrain bundle.

Other invasive therapies, such as cingulotomy and capsulotomy also aimed at disrupting connectivity from frontal regions by lesioning white-matter bundles[21]. It could recently be shown that such tract- or network-based concepts may be used to predict clinical improvements across DBS centers and surgeons for the case of Parkinson's disease[22,23]. Based on modern neuroimaging methods and high-resolution connectomic datasets, connectivity of DBS electrodes to specific cortical regions was associated with stronger therapeutic effects in various diseases treated with this surgical procedure[22,24–26].

For the case of OCD, Baldermann et al.[24] recently demonstrated that structural connectivity from DBS electrodes to medial and lateral prefrontal cortices was associated with stronger symptom alleviation. Crucially, they were also able to identify a specific subsection of the ALIC that was highly associated with symptom improvements after one year of DBS. Of note, connectivity to this fiber tract was able to predict ~40% of the variance in clinical outcome in out-of-sample data. The bundle connected to both medial dorsal nucleus of the thalamus and to the anterior part of the STN (which have received substantial attention in the context of OCD). The STN itself is a prominent target for DBS of various diseases including PD, dystonia, OCD and Tourette's syndrome[27]. The small nucleus receives widespread direct afferents from most parts of the prefrontal cortex and is involved in motor, associative and limbic processing[28]. Due to these spatially organized cortico-subthalamic projections, the nucleus has functional zones that largely follow the organization of the frontal cortex, i.e. sensorimotor parts of the STN are situated posterior, followed by pre-/oculomotor-, associative and limbic domains in anteromedial direction.

Consequently, the anterior (associative/limbic) parts of the STN have been targeted by DBS for OCD[29]; these same anterior subregions were exclusively connected to the tract target identified by Baldermann et al.[24] in ALIC-DBS patients. Following up on this, our present study aimed at testing whether the same tract could be associated with good clinical outcome in a cohort treated with STN-DBS. We retrospectively analyzed two cohorts of DBS patients that were treated with either STN-DBS or ALIC-DBS in order to test our hypothesis, that the same tract could potentially predict clinical improvement in STN-DBS as well as ALIC-DBS. In this attempt, we identified a common tract that already became apparent when analyzing either cohort alone. After calculating the tract exclusively based on data of one cohort (e.g. ALIC), we cross-predicted outcome in the other cohort (e.g. STN), and vice versa. We then tested predictive utility of this tract in two additional cohorts from a third and fourth center. Finally, we set the resulting tract target into the larger context of OCD-DBS literature and tested, whether it could be used to explain outcomes of reported clinical studies with different surgical targets.

Results

Clinical results. Two cohorts (Cologne; ALIC target; $N = 22$; and Grenoble; STN target; $N = 14$, two electrodes in each patient) formed a training and cross-validation sample in which the tract target was identified and validated. Each of the two cohorts were first analyzed independently, then used to cross-predict outcome in patients from the other one. The main part of our analyses focuses on these two cohorts. As further validation of results, two additional test cohorts were included (Madrid: two electrodes in each patient targeting bilateral nucleus accumbens (NAcc); London: four electrodes in each patient targeting bilateral ALIC and STN).

Patients in all cohorts were of similar age with a similar Y-BOCS score at baseline and comparable Y-BOCS improvement scores (Table 1). In the first test cohort (Madrid; NAcc target; $N = 8$), improvement scores were taken after activating each of the four electrode contact pairs for 3 months, respectively (following the clinical protocol described in ref. [30]). This resulted in a total of 32 data points. In the second test cohort (London; both ALIC and STN target; $N = 6$, four electrodes in each patient), stimulation parameters resulted from an optimized phase following parameter optimization.

Electrode localization confirmed accurate placement to each of the three target regions for all patients of the four cohorts (Fig. 1).

Connectivity analysis. Connectivity analysis results seeding from electrodes of the two training cohorts (Cologne and Grenoble) based on the $N = 985$ HCP normative connectome are shown in Fig. 2. The overall connectivity of electrodes to other areas in the brain (without weighing for clinical improvement) was strikingly different between the two cohorts (Fig. 2, top row). This is hardly surprising as it mainly reflects the overall structural connectivity profiles of the two DBS targets. The STN as a widely connected basal-ganglia entry point and the ALIC as a white-matter structure are differently connected in the brain. However, when tracts were weighted by their ability to discriminate between good and poor responders (using the fiber T-score method described

Table 1 Patient demographic details and clinical results of the two cohorts.

	ALIC-DBS cohort (mean ± SD)	STN-DBS cohort (mean ± SD)	NAcc DBS cohort (mean ± SD)	Combined DBS cohort (mean ± SD)
Center	University Hospital Cologne	University Hospital Grenoble	Hospital Clínico San Carlos Madrid	University Hospital London
Reference(s)	[22, 31]	[28]	[40]	[16]
N of patients (females)	22 (12)	14 (9)	8 (4)	6 (1)
N of electrodes	44	28	16	24
Age	41.7 ± 20.5	41 ± 9	35.3 ± 10.4	45.5 ± 10.5
Y-BOCS baseline	31.3 ± 4.4	33.4 ± 3.7	30 ± 7.75	36.2 ± 1.8
Y-BOCS after DBS	20.7 ± 7.7 (12 months postop)	19.6 ± 10.6 (12 months postop)	14.75 ± 7.2 (3 months postop of best contact)	14.3 ± 4.1 (optimized phase in ref. [16])
Absolute Y-BOCS Improvement	9.6 ± 6.5	13.8 ± 10.8	15.1 ± 9.6	21.83 ± 5.7
% Y-BOCS Improvement	31.0 ± 20.5%	41.2 ± 31.7%	47.8 ± 23	50.0 ± 12.6%

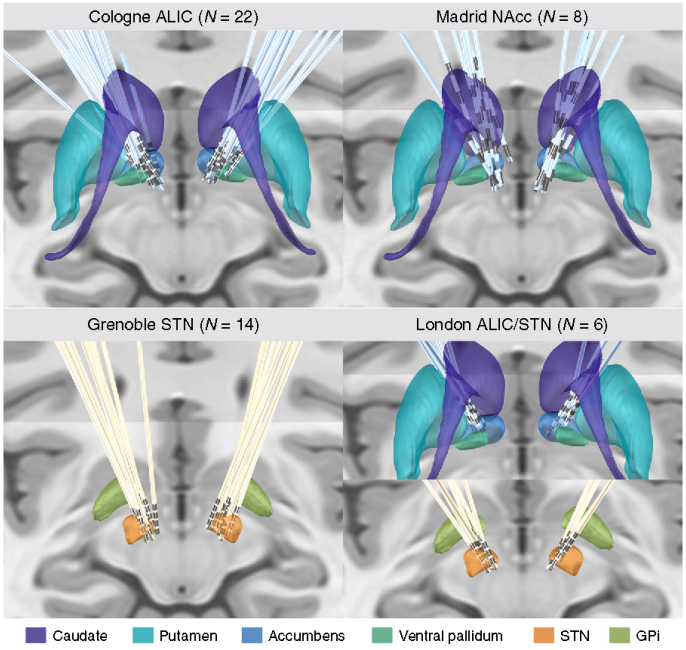

Fig. 1 Overview of lead electrode placement. The two training/cross-validation cohorts (left) targeting ALIC (Cologne) and STN (Grenoble), and the two test cohorts (right) targeting NAcc (Madrid) and both ALIC & STN with four electrodes per patient (London) are shown. Subcortical structures defined by CIT-168 Reinforcement Learning Atlas[63] (ALIC/NAcc region) and DISTAL Atlas[64] (STN region), with coronal and axial planes of the T1-weighted ICMB 152 2009b nonlinear template as background.

below), a positively discriminative tract to the medial prefrontal cortex emerged in each cohort even when cohorts were analyzed independently (Fig. 2, middle row). The degree of lead connectivity to this tract correlated with clinical improvement ($R = 0.63$ at $p < 0.001$ in the ALIC cohort and $R = 0.77$ at $p < 0.001$ in the STN cohort; Fig. 2, bottom row).

Of note, these correlations are somewhat circular and meant to describe the degree of how well discriminative tracts could explain the same sample of patients on which they were calculated. More interestingly, in the next step, the tract was calculated exclusively on data from the STN cohort and then used to explain outcome in the ALIC cohort ($R = 0.50$ at $p = 0.009$) and vice versa ($R = 0.49$ at $p = 0.041$; Fig. 3).

Crucially, some VTAs of the ALIC cohort resided entirely below the identified tract and thus received a fiber T-score of (near) zero (also see blue example patient in Fig. 3, bottom right). The same holds true when either calculating the tract based on the STN cohort (Fig. 3) or the ALIC cohort itself (Fig. 2). To further investigate this matter, two-sample t-tests between improvements of patients with near-zero scores (fiber T-scores below 50) and the remaining patients with VTAs covering the tract well (scores above 50) were calculated. This showed that

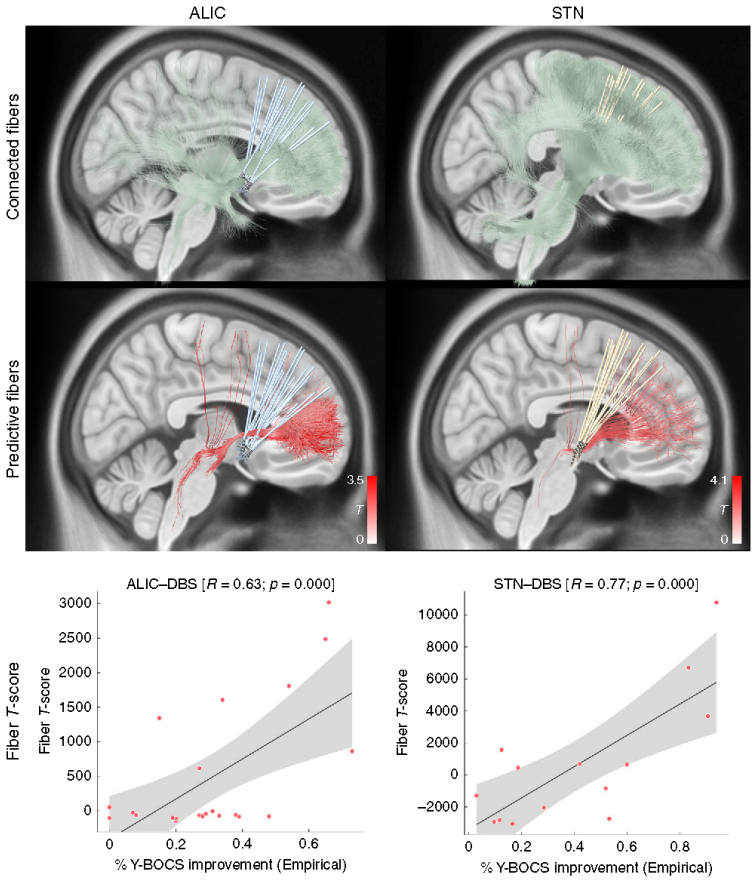

Fig. 2 Predictive fiber tracts in training cohorts. Top: all fibers connected to the sum of volumes of tissue activated (VTAs) of each cohort are shown in green. Middle: predictive fibers positively associated with clinical improvement are shown in red. Only positive fibers are shown here for reasons of clarity. See Fig. 3 for negatively associated tracts. The top 20% predictive fibers are displayed. Bottom: correlations between the degree of stimulating positively predictive tracts (sum of aggregated fiber *T*-scores under each VTA) and clinical improvements. Gray shaded areas represent 95% confidence intervals. This analysis is based on a normative connectome, a replication of it based on anatomically predefined pathways is shown in Supplementary Fig. 1.

VTAs with large overlap with the tract resulted in significantly better clinical improvement ($T = 6.0$ at $p < 10^{-5}$ when the tract was calculated on the ALIC cohort, Fig. 2, and $T = 3.7$ at $p < 0.005$ when it was calculated on the STN cohort, Fig. 3).

Depending on the target, the analysis revealed different proportions of "positive" and "negative" fibers (ALIC cohort: 22.2k positive vs. 1.9k negative fiber tracts selected from the group connectome; STN cohort: 45.1k positive vs. 48.6k negative fibers and both cohorts combined: 54.4k positive vs. 9.6k negative fibers).

Replication on independent test cohorts. In the next step, the analysis was performed on the two cohorts combined. Again, the same tract emerged, now even more clearly (Fig. 4, top). Bundles were selected from the connectome and visualized, that were predominantly connected with VTAs of patients from both cohorts with good (red) or poor (blue) improvement, respectively. The resulting positive discriminative tract traversed slightly dorsal to the group of electrodes of the ALIC cohort and coursed centrally or slightly ventral to the electrodes of the STN cohort. This tract was then used to predict outcome in two independent test cohorts of patients that underwent surgery in a third and fourth center (Madrid & London; Fig. 4, bottom). Although the surgical target of the Madrid cohort was the NAcc, electrode placement was comparable to the ALIC/Cologne cohort (Fig. 1). Here, improvements were taken for each contact pair that had been switched on during a 3-month interval, leading to 32 data points (Fig. 4, bottom left, active contact pair color coded). In the London cohort, patients had received two electrodes to each target (four in total) and fiber *T*-scores scores were summed up across targets. In both test cohorts, stimulation overlap with the tract target significantly correlated with empirical improvement (Madrid: $R = 0.50$ at $p < 0.001$, London: $R = 0.75$ at $p = 0.040$). Of note, VTAs in the London sample were estimated with a different software (see Methods), patients received four electrodes and the clinical scores represented an "optimized" phase following 9 months of a clinical trial[13].

Given the high amount of false-positive connections present in dMRI-based connectomes[31], we replicated all findings of the

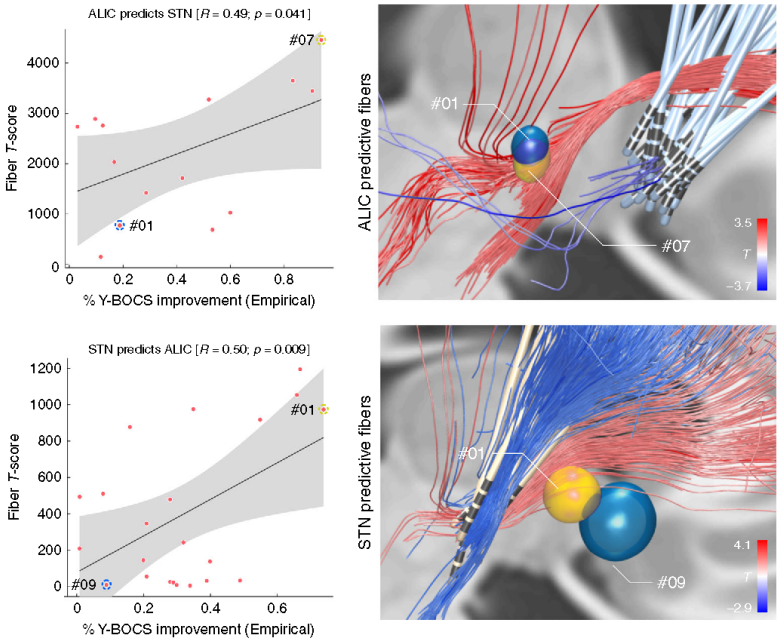

Fig. 3 Cross-prediction between ALIC and STN training cohorts. Top: when the tract was calculated exclusively based on data from the ALIC cohort, it was used to calculate fiber *T*-scores for all patients in the STN cohort. These were correlated with clinical improvements in the STN cohort. One example patient with strong overlap of the tract (yellow) received a high fiber *T*-score, whereas one with less overlap received a lower score (blue). The two example patients are marked in the correlation plot on the left. Bottom: here, the tract was calculated exclusively on data from the STN cohort to predict outcome in patients in the ALIC cohort. Again, two example patients are shown. Gray shaded areas in the correlation plots represent 95% confidence intervals. Of note, here, some VTAs barely overlapped with the tract (as the blue example VTA) and consequently received a near-zero score.

study using a synthesized anatomical atlas that is based on established anatomical knowledge[17] and thus free of such false-positive connections. Results were highly similar and identified the hyperdirect pathway connecting the dorsal anterior cingulate cortex (dACC) to the STN to be most associated with clinical outcome (Supplementary Figs. 1 and 2).

A tract target for OCD-DBS. The tract target identified here may potentially "unify" some aspects of the STN and ALIC/NAcc targets for OCD. Thus, in a final analysis, we aimed at setting it into context with other DBS targets that were used in OCD-DBS, before. To do so, we converted literature-based targets into template space[32] and set them into relation with the tract target (see Fig. 5, Table 2 and Supplementary Methods). A large number of reported DBS targets for OCD seemed to cluster on or around the tract. Furthermore, clinical improvement values that had been reported in these studies could be significantly accounted for by calculating the weighted overlap between stereotactic target sites and the tract (Fig. 5c, see Supplementary Methods for details).

Given the potential clinical importance of the identified tract, we estimated a final version of the tract based on all four cohorts and characterized its anatomical properties using additional views relative to anatomical landmarks (Fig. 6 and Supplementary Fig. 3). Anatomically, the tract is a subpart of the well-characterized ALIC that connects areas of the prefrontal cortex with the subthalamic nucleus and MD nucleus of the thalamus[33,34]. Anatomical validity of the isolated tract was discussed with four anatomists and further experts in the field (see Acknowledgements section). In the motor domain, the "hyperdirect pathway", i.e., a direct connection from frontal cortex to subthalamic nucleus, has been well established[35,36], functionally, but the STN is known to receive widespread and direct input from widespread areas of the prefrontal cortex[33]. Thus, the main part of the specific bundle delineated here may represent a route of direct input from frontal regions to the STN. In addition, connections between mediodorsal nucleus of the thalamus and prefrontal regions received slightly lower (but positive) *T*-scores and are not shown in 3D visualizations but well visible in 2D sections shown in Fig. 6. The bundle most negatively associated with clinical improvement was the posterior limb of the anterior commissure, connecting bilateral temporal cortices.

To properly define the anatomical course of this tract, we openly released it as an atlas in stereotactic (MNI) space within Lead-DBS software (www.lead-dbs.org). Of note, Lead-DBS is scientific and not clinical software and the tract should not be vacuously used for any form of clinical decision making[37].

Discussion

We analyzed data from four cohorts of OCD patients with different DBS targets using a connectomic approach. Strikingly, the same optimal tract target emerged when separately analyzing either an ALIC-DBS or STN-DBS cohort, alone. Among other regions, this bundle connected dorsal anterior cingulate and ventrolateral prefrontal cortices to the anteriomedial STN. When the tract was calculated on either cohort alone, it could be used to cross-predict clinical improvement in the other cohort, respectively. Furthermore, variance in clinical outcomes in two independent test cohorts from a third and fourth center could be

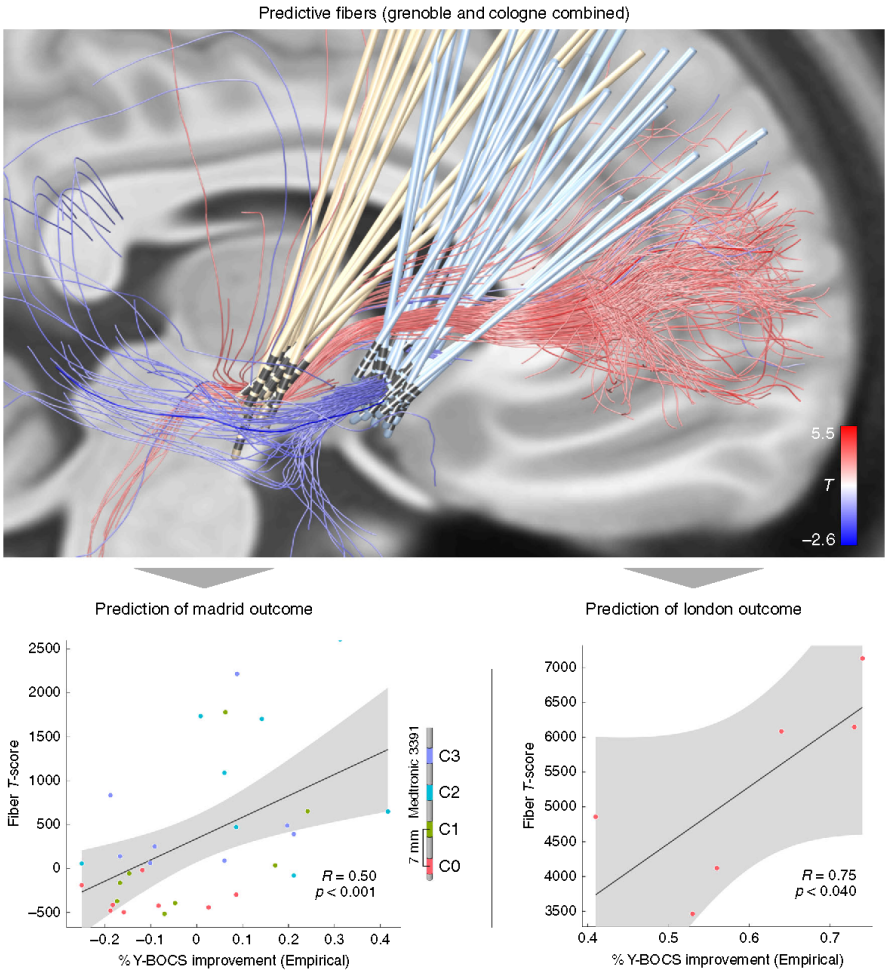

Fig. 4 Predictions in test cohorts. Top: predictive fibers calculated on both training cohorts (Cologne & Grenoble) irrespective of their target. Red fibers are positively associated with clinical improvement, blue fibers negatively. Bottom: the sum of aggregated fiber *T*-scores under each VTA predicted %-Y-BOCS improvements in eight patients with four settings each ($N = 32$ stimulations) of the Madrid cohort (left) and six patients of the London cohort with dual stimulation (four electrodes) of STN and ALIC (right). Gray shaded areas represent 95% confidence intervals. Please note that p-values in this manuscript are based on random permutation testing. Based on classical tests, the result shown in the lower right panel would remain significant in a one-sided test, only (p-one-sided = 0.044, p-two-sided = 0.089). A replication of this result based on anatomically predefined pathways is shown in Supplementary Fig. 2.

significantly predicted based on stimulation overlaps with the tract. Finally, literature-based stimulation sites for OCD seemed to cluster close to the identified tract. Indeed, their spatial proximity to the tract correlated with reported clinical improvements across studies.

The subthalamic nucleus receives afferents from a large portion of the prefrontal cortex by hyperdirect pathways that are known to traverse within the internal capsule[33,38]. In rodents, lesions to such a "limbic hyperdirect pathway" led to diminished discriminative accuracy and increased perseveration[39]. One classical cortical region, which was described as an origin of limbic hyperdirect input is the dACC[17,33,40], which has a prominent role in the classical cortico-striato-thalamo-cortical (CSTC) model of OCD[40] and leads to improvement of OCD symptoms when directly lesioned in humans[41]. The normative connectome analysis identified the dACC as a cortical connection site to the identified tract, among others. Because of the high amount of false-positive connections in diffusion MRI-based connectomes[31,42], we repeated the analysis using an atlas of predefined anatomical tracts[17]. Here, the hyperdirect pathway connecting dACC to the STN was isolated as the only of five bundles in the ALIC that were included in the atlas (Supplementary Figs. 1 and 2). Thus, hyperdirect cortical input from dACC to STN could be an anatomical and functional substrate of the identified bundle. In this context, it is crucial to note that the atlas by nature cannot represent each and every white-matter

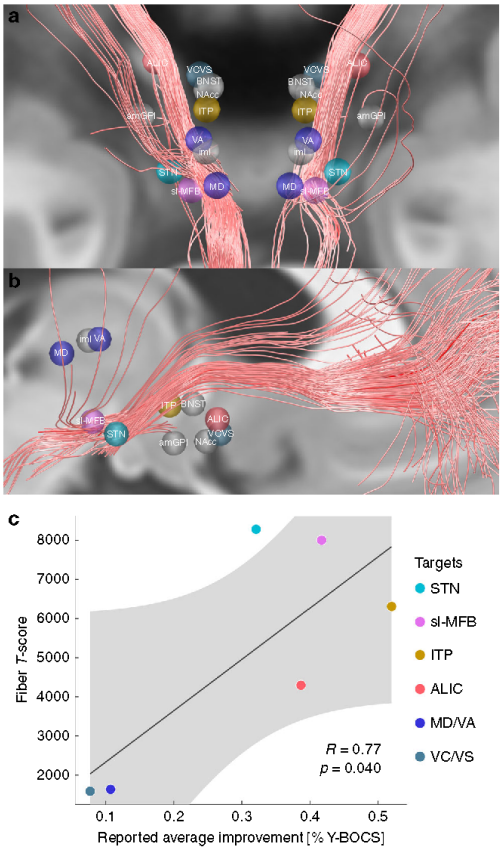

Fig. 5 Literature defined OCD targets in relationship to the identified tract. Overview of the positively predictive fiber tracts identified in the present study are shown in synopsis with DBS targets for treatment of OCD from reported studies. Note that most targets were reported for the tip of the electrode, thus, active stimulation may have occurred dorsal to shown targets (Table 2). **a**, **b** Reported average targets mapped to standard space. **c** The degree of weighted overlap between stimulation sites and the identified tract. These were correlated with reported average %-Y-BOCS improvements of published studies (where available, other sites marked in gray; see Supplementary Methods for details). Gray shaded area represents 95% confidence intervals.

bundle that exists in the ALIC / STN region and shows "gaps" in between the included bundles (Supplementary Figs. 1 and 2). Thus, while normative connectomes include a large number of false-positive fibers, the atlas may instead be prone to false-negative connections, as some tracts are simply not included. For instance, it is known that the STN receives direct input from other areas of the prefrontal cortex such as the ventrolateral prefrontal cortex[43]. In summary, although dACC and vlPFC are likely candidates to play a functional role, our methods and results are unable to determine the exact cortical region(s) of origin with absolute certainty. Despite this limitation, our results define a precise three-dimensional reconstruction of the tract itself (i.e. a definition of where it exactly traverses within the ALIC) in standard stereotactic space.

A highly similar pathway that already served as a tract target in an $N = 2$ case-series of OCD patients[10] also traversed within the ALIC but has instead been referred to as the superolateral branch of the medial forebrain bundle (slMFB)[37]. The original anatomical definition of the medial forebrain bundle suggests a more ventral route connecting the ventral tegmental area to the olfactory cortex while bypassing the red nucleus laterally[34]. In other words, the anatomical definition of the medial forebrain bundle does not traverse within the ALIC. This mismatch between the surgical target (slMFB) and anatomical literature (mfb) has recently been confirmed by the original authors of the surgical target and they now referred to it by vtaPP (for ventral tegmental area projection pathway)[44]. This potentially misleading nomenclature of the surgical slMFB target has suggested that results in two previous OCD studies would be conflicting, while anatomically, their results agreed. Both studies favored a similarly defined tract within the ALIC, which was referred to as slMFB in one study[45] and as anterior thalamic radiation in the second[24]. To readers, this suggested conflicting results while they were in fact confirmatory (based on the location of both tracts within the ALIC). Thus, we welcome the recent steps taken to move away from calling the surgical target slMFB toward calling it vtaPP[44]. This said, our interpretation of the identified tract differs. Our findings reveal a tract connecting frontal areas with the STN (cf. Supplementary Fig. 3C and results from the basal-ganglia pathway atlas, Supplementary Figs. 1 and 2). Thus, we attribute the tract to afferents of the STN (limbic hyperdirect pathway) as opposed to efferents of the ventral tegmental area implied by the term vtaPP[44].

This interpretation is supported by combined analyses of dMRI and tracing methods in nonhuman primates as well as human subjects, which were used to segregate prefrontal fibers passing through the internal capsule[46]. Fibers that originated from ventrolateral prefrontal cortices (areas 45 and 47) were shown to terminate in the medial part of the STN and the MD nucleus of the thalamus—precisely corresponding to the tract described here. Alternatively—or additionally—the hyperdirect pathway projecting from dACC to the STN may be functionally involved in mediating treatment outcome. As mentioned, a strong additional hint for this latter hypothesis is that lesions to the dACC itself have beneficiary effects on OCD[41].

Based on our results, two testable hypotheses with implications above and beyond OCD could be proposed. First, different surgical targets may reduce the same symptoms equally well—potentially by modulating the same tract or network. Second, in addition, they may modulate not only one (shared) network but other networks that are not shared, resulting in different changes across other behavioral domains. This can be seen by widely different connectivity profiles of the targets (Fig. 2, top row) and differential effects of STN vs. ALIC stimulation on depressive/cognitive functions described by Tyagi et al.[13]. Thus, one may speculate that networks are symptom-specific (and not disease-specific). When modulated, these networks or tracts seem to not ameliorate a specific disease but rather specific symptoms present in the disease.

In OCD, accordingly, different symptom types (for example contamination vs. checking) were found to activate different prefrontal sites (ventromedial vs. dorsolateral, respectively)[47]. Similar observations were made in other diseases, before. For instance, Akram and colleagues demonstrated that connectivity to specific cortical regions was associated with improvement in different clinical features of Parkinson's disease (e.g. connectivity to M1 preferentially reduced tremor while to the SMA reduced rigidity and bradykinesia)[25]. Similarly, connectivity from electrodes to M1 was associated with tremor improvement in Essential Tremor[48].

Table 2 DBS targets for treatment of OCD defined in the literature.

DBS target	References	Number of patients	% Y-BOCS change	AC/PC coordinates	Relative to	Target type	MNI coordinates (Fig. 5)
STN	Mallet et al.[66]	8	32.1	NA	AC	Tip of the electrode	±11.30 −9.90 −7.81
amGPi	Nair et al.[9]	4[a]	NA	±14.47 9.85 −3.28	MCP	Tip of the electrode	±15.66 −1.41 −8.22
VC/VS	Tsai et al.[67]	1	7.7	±7.5 16.3 −3.05	MCP	Tip of the electrode	±7.92 5.51 −9.01
slMFB	Coenen et al.[10]	2	41.7 (at 12 months)	±7.6 −1.72 −3.0	MCP	Active contacts	±8.35 −13.64 −7.00
NAcc	Sturm et al.[5]	4	NA	±6.5 2.5 −4.5	AC	Tip of the electrode	±6.98 3.69 −10.55
ALIC	Nuttin et al.[68]	6	38.7	±13 3.5 0	AC	Tip of the electrode	±13.84 5.17 −5.04
MD	Maarouf et al.[11]	4	10.7	±4.7 −18.52 4.87	AC	Active contacts	±5.10 −18.17 2.59
VA	Maarouf et al.[11]	4	10.7	±6.84 −13.76 7.78	AC	Active contacts	±7.52 −12.68 5.60
iml	Maarouf et al.[11]	4	10.7	±5.78 −14.9 7.08	AC	Active contacts	±6.36 −13.99 4.85
ITP	Lee et al.[69]	5	52.0	±6.5 −3 −0.5	AC	Tip of the electrode	±6.92 −1.84 −5.13
BNST	Nuttin et al.[70]	4	NA	±6 0 0	AC	Tip of the electrode	±6.33 1.39 −4.87

MD medial dorsal thalamic nucleus, *VA* ventral anterior thalamic nucleus, *iml* internal medullary lamina, *MCP* mid-commissural point, *AC* anterior commissure.
[a]Tourette patients, with prominent symptoms of OCD.

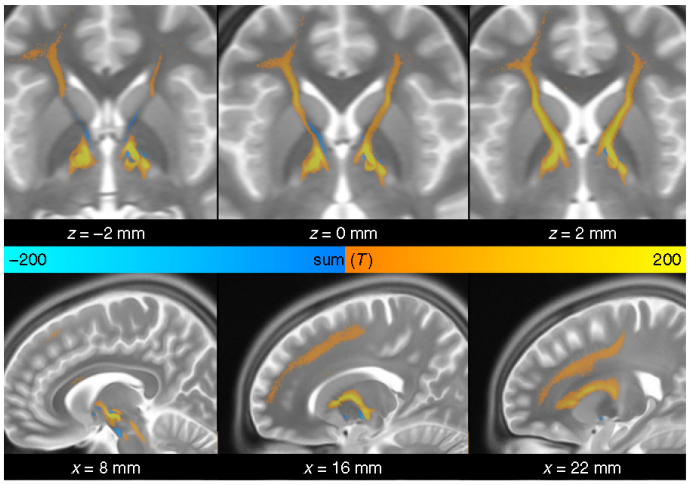

Fig. 6 Anatomical course of discriminative fibers shown in MNI space. The tract is connected to the subthalamic nucleus and mediodorsal nucleus of the thalamus, traverses through the anterior limb of the internal capsule and has a wide array of frontal connections including dorsal anterior cingulate cortex and ventrolateral prefrontal cortex. The tract most negatively associated with clinical improvement was the anterior commissure.

Supporting the first hypothesis, our study was able to predict symptom-specific clinical improvement across DBS targets and centers based on connectivity data. Although the tract that our data seems to shape out is predictive for Y-BOCS improvement, different tracts could have emerged when repeating the analyses for depressive or cognitive flexibility symptoms (as analyzed by Tyagi et al.[13]).

Going further, shared symptom networks could be present in other diseases for which multiple surgical targets are investigated. Major depression and Tourette's syndrome are obvious examples and extensive work in this direction is currently ongoing[14,49,50]. Similar concepts could even be applied to more established targets such as STN vs. GPi DBS[51] or symptom-specific alleviations across diseases.

Potentially, DBS surgery in the (distant) future could involve detailed preoperative phenotyping to establish a broad patient-specific symptom score. Based on databases of clinical improvements along affected symptom axes, a mix of networks that should be modulated to alleviate each patient's specific symptom profile could be identified. Such concepts are still mostly speculation but could be investigated in future studies. This said, we must emphasize that the present study investigated data on a group level and utilized connectivity data from individuals without OCD. As mentioned by others in the very context, we could not agree more that surgical decision making for DBS should not be based on such aggregated normative data, alone[37]. Further studies are required to determine whether individual patient connectivity or generic connectome data (or both) could assist with optimizations in surgical targeting or DBS programming by determining crossing sites of symptom networks for specific patients.

Several limitations apply for the current work. First and foremost, the retrospective character of the study is not ideal to compare and study effects of clinical outcome which is why we kept clinical information to a minimum and instead referred to the underlying clinical studies.

Second, it has been shown that dMRI-based tractography reconstructs a very high proportion of false-positive fibers in recent open challenges[31,42]. We aimed at reducing the risk of false-positive tractography results in four ways. First, we used the tracking method that achieved the highest (92%) valid connection score among 96 methods submitted from 20 different research groups in a recent open competition[31]. Second, we used highest quality multi-shell diffusion data[52] acquired on a high N (985 subjects) at a state-of-the-art imaging center (HCP data acquired at Washington University in St. Louis, see Acknowledgements). Third, we compared the tract results with anatomy text-books and discussed its validity with four anatomists (see Acknowledgements). Fourth, we replicated findings based on an atlas that is based on predefined anatomical tracts (Supplementary Methods). The tract described in the present study matches results from this atlas (Supplementary Figs. 1 and 2). However, the potential that the tract represents a false-positive result may not be completely ruled out given the fundamental limitations of dMRI-based tractography[31,42].

Third, we used normative connectome data instead of patient-specific diffusion-weighted MRI data (which is not available for most of the patients included). This poses marked limitations as such data cannot be representative of patient-specific anatomical variations. Still, we argue that some aspects about general pathophysiological mechanisms may be investigated using normative data and robust cross-validations across cohorts shown here suggest this holds true. Use of normative connectomes has been introduced in other clinical domains where patient-specific MRI data is unavailable, such as stroke[53,54] or transcranial magnetic stimulation[55]. In DBS, the technique has been applied before and has led to models that could be used to predict improvements in out-of-sample data[22,24]. In addition to the practical advantage of being applicable to cases where patient-specific data is lacking, normative data also has the theoretical advantage of better data quality. In the present case, a connectome dataset was derived from a high N of 985 subjects scanned under research conditions by a specialized imaging center[52]. It may be logistically challenging to acquire data of such quality in a clinical routine setting (e.g. pre-operatively) in individual patients but could be feasible in specialized centers. Still, studies have pointed out that tractography-based DBS targets pointed to coordinates that were sometimes >2 mm apart from each other when repeating analyses on test–retest scans of the same subject[56]. Similarly, variance introduced by single subject scans was too high to be useful in a test–retest study that aimed at creating clinically useful and robust thalamic DBS targets[57]. However, patient-specific connectivity can never be reconstructed when using normative connectomes. Thus, normative connectomes will likely not embody the final solution to the connectomic surgery framework and will be challenged by advances in MRI technology and algorithm developments. Potentially, as a step in-between, using combined information from normative and patient-specific connectomes could embody a promising strategy that should be explored, in the future.

Fourth, inaccuracies in lead localization may result from the approach of warping electrodes into common space as done here. To minimize this issue, we used a modern neuroimaging pipeline that has been scientifically validated in numerous studies and involved advanced concepts such as brain shift correction[58], multispectral normalization, subcortical refinement[58] and phantom-validated electrode localizations[59]. The normalization strategy that was applied was found to automatically segment the STN as precisely as manual expert segmentations[60] and each step of the pipeline was carefully assessed and corrected if needed by a team with long-standing expertise in this area[58,61]. Besides, both post-operative CT (33 patients) and post-operative MRI (17 patients) were used for electrode localization in the current dataset. Although studies have reported similar agreement between the results based on the two modalities, this might still lead to slight inconsistencies across patients. A larger dataset acquired with a homogeneous protocol would be ideal to validate our results, in the future.

Finally, given the correlative nature of the study, our findings may not differentiate between local and global effects. For instance, the tracts may have spuriously originated in the ALIC group because a more dorsal stimulation resulted with better clinical outcome. The congruency between results derived from STN- and ALIC-cohorts resulting in the same fiber bundle still suggests that the identified tract could play a causal role. However, such a claim would need to be confirmed e.g. using optogenetics or electrophysiology.

Four main conclusions may be drawn from the present study. First, we show that the overall connectivity profiles of STN- and ALIC-DBS electrodes project to largely different areas in the brain. Second, data in each target alone singled out the same fiber bundle that was associated with long-term improvement of OCD symptoms when modulated either at level of the STN or the ALIC. Third, we demonstrated that it is possible to cross-predict clinical improvement of OCD patients across DBS target sites (ALIC/STN) and centers (Cologne/Grenoble). Finally, we confirm results by predicting outcome in two additional cohorts from different centers (Madrid/London) and set results into context of published reports.

Methods

Patient cohorts and imaging. Fifty OCD patients from four centers were retrospectively enrolled in this study, among them 22 patients from University Hospital of Cologne implanted for ALIC-DBS, 14 patients from Grenoble University Hospital who underwent STN-DBS surgery, 8 patients who received bilateral electrodes targeting the NAcc from Hospital Clínico San Carlos in Madrid and 6 patients who received electrodes to both STN and ALIC from the National Hospital for Neurology and Neurosurgery in London. The patients from Cologne, Grenoble and Madrid received two electrodes each ($N = 44$ patients with $N = 88$ electrodes), the six patients in the London cohort received four electrodes each ($N = 6$ patients with $N = 24$ electrodes). All patients from Grenoble were bilaterally implanted with DBS electrodes 3389, as were all but three patients from Cologne, who received type 3387 electrodes (Medtronic, Minneapolis, Minnesota, US). Patients from London received models 3389 to the STN and 3387 to the ALIC. Patients from Madrid received models 3391. All patients qualified for DBS surgery based on their diagnoses of treatment-resistant severe OCD[13,24,29]. Severity of OCD was assessed both pre- and postoperatively using the Yale-Brown Obsessive-Compulsive Scale (Y-BOCS). Post-operative assessment took place 12 months after surgery in Cologne, Grenoble and London cohorts. In case of the London cohort, this followed a four-step clinical trial (2 × 3 months blinded stimulation at one target followed by 6 months of stimulation at both targets, the last 3 months using clinically optimized parameters. For details see ref. [13]). In the Madrid cohort, each of the four contact pairs was activated for 3 months, with a 1-month wash-out period between trials and a 3-month sham period. In our analysis, this led to 32 data points (i.e. stimulation-based outcomes). Patients' demographic details are provided in Table 1. All patients gave written informed consent. The protocols were approved by the Ethics Committee of each center, respectively. The current study was further approved by the local ethics committee of Charité—University Medicine Berlin in accordance with the Declaration of Helsinki.

For all patients in the four cohorts, high-resolution structural T1-weighted images were acquired on a 3.0-Tesla MRI scanner, before surgery. Post-operative computer tomography (CT) was obtained in thirty-three patients after surgery to verify correct electrode placement, while 11 patients from the Grenoble cohort and the six London patients received post-operative MRI instead. Post-operative MRI parameters were as follows. Grenoble cohort: T1-weighted 3D-FFE scans were acquired on a 1.5 T Philips MRI scanner with a $1.0 \times 1.0 \times 1.5$ mm^3 voxel size; TR: 20 ms, TE: 4.6 ms, flip angle: 30 deg. London cohort: T1-weighted 3D-MPRAGE scans were acquired on a 1.5 T Siemens Espree interventional MRI scanner with a $1.5 \times 1.5 \times 1.5$ mm^3 voxel size and three-dimensional distortion corrected using the

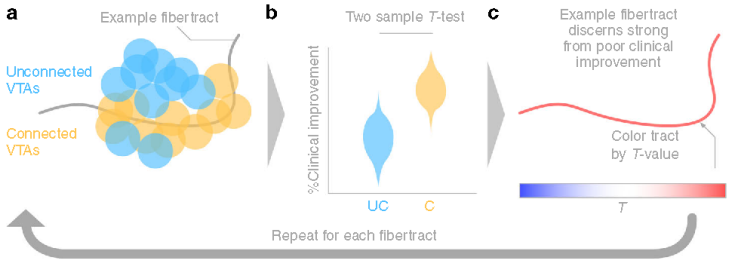

Fig. 7 Summary of methods to define a *T*-value for each tract. a For each fiber, VTAs were grouped into either connected (C; yellow) or unconnected (UC; blue) sets across patients. **b** Two-sample *t*-tests between clinical improvements in connected and unconnected VTAs were calculated in a mass-univariate fashion for each fiber tract separately. **c** The resulting *T*-value of this analysis leads to the "weight" that each fiber received, as well as the color in visualizations throughout the manuscript. Here, red means that the fiber tract is favorably connected to good responders, whereas blue indicates the opposite (and the saturation of tracts denotes how discriminative they are).

scanner's built-in module; TR: 1410 ms, TE: 1.95 ms, FOV: 282 mm, flip angle: 10 deg, acquisition time 4 min and 32 s, relative SNR: 1.0.

DBS lead localization and VTA estimation. DBS electrodes were localized using Lead-DBS software (http://www.lead-dbs.org)[58]. Post-operative CT and MRI scans were linearly coregistered to preoperative T1 images using Advanced Normalization Tools (ANTs, http://stnava.github.io/ANTs/)[62]. Subcortical refinement was applied (as a module in Lead-DBS) to correct for brain shift that may have occurred during surgery. Images were then normalized into ICBM 2009b Nonlinear Asymmetric ("MNI") template space using the SyN approach implemented in ANTs, with an additional subcortical refinement stage to attain a most precise subcortical alignment between patient and template space ("Effective: Low Variance" preset as implemented in Lead-DBS). This specific method was top performer for subcortical image registrations in a recent comparative study that involved >10,000 nonlinear warps and a variety of normalization techniques[60]. Both coregistrations and normalizations were visually reviewed and refined, if needed. DBS electrodes were then localized using Lead-DBS and warped into MNI space.

In the Grenoble, Cologne and Madrid groups, VTA were estimated using a finite element method (FEM)[58]. A volume conductor model was constructed based on a four-compartment mesh that included gray matter, white matter, electrode contacts and insulated parts. Gray matter was defined by the CIT-168[63] and DISTAL[64] atlases for the ALIC-/NAcc and STN-cohorts, respectively. These atlases were specifically adapted or created for use within the Lead-DBS pipeline. The electric field (E-field) distribution was then simulated using an adaptation of the FieldTrip-SimBio pipeline that was integrated into Lead-DBS (https://www.mrt.uni-jena.de/simbio/; http://fieldtriptoolbox.org/) and thresholded at a level of 0.2 V/m[58].

For the London test cohort, we chose to use the original VTAs of the published study by Tyagi et al.[13]. These had instead been processed using Medtronic SureTune™ software and transferred into MNI space within the original study. The reason we chose to use the original VTAs were twofold. First, it would demonstrate generalizability of our findings (i.e. that our results could still be useful in case electrodes were localized using different software). Second, we aimed at yielding maximal transferability to the study by Tyagi et al.[13], which reported on the rich London dataset in more depth.

Connectivity analysis. Structural connectivity between VTAs and all other brain areas was calculated based on a normative connectome as similarly done in previous work[22,24,32,58,64]. Specifically, a whole-brain connectome based on state-of-the-art multi-shell diffusion-weighted imaging data from 985 subjects of the Human Connectome Project (HCP) 1200 subjects data release[52] was calculated in each patient using Lead-Connectome (www.lead-connectome.org). Whole-brain fiber tracts were normalized into standard space using a multispectral warp based on T1-weighted, T2-weighted, and diffusion-weighted acquisitions using ANTs (using the same "Effective Low Variance" preset implemented in Lead-DBS). In each subject, a total of 6000 fibers were sampled and aggregated to a joint dataset in standard space, resulting in a set of 6,000,000 fibers across 985 HCP subjects. For each of these tracts, a "Fiber *T*-score" was assigned by associating the fiber tract's connectivity to VTAs across patients with clinical outcome (Fig. 7). Specifically, (mass-univariate) two-sample *t*-tests between clinical outcomes in connected and unconnected VTAs were performed for all 6,000,000 tracts. Needless to say, these *T*-scores were not meant to result in significant results (given the mass-univariate nature of tests) but instead formed a model that could be used for out-of-sample predictions in other DBS cohorts. *T*-values from these tests should be seen as "weights" and could be positive or negative (since two-sided *t*-tests were performed). A high absolute *T*-value meant that the fiber was strongly discriminative between good and poor responding VTAs or predictive for clinical outcome. For instance, a tract that was connected exclusively to VTAs in good responders (and not to VTAs of poor responders) would receive a high positive score. In return, a patient would most likely show more pronounced clinical benefit, if her/his VTA was strongly connected to many fibers with high positive *T*-values but not too many with negative scores. This analysis made it possible to assign aggregated fiber *T*-scores to each (out-of-sample) VTA in subsequent prediction analyses.

To account for the fact that larger VTAs would potentially automatically receive higher fiber *T*-scores, these were divided by the stimulation amplitude throughout the manuscript. Finally, Monte-Carlo random permutations (×1000) were conducted to obtain *p*-values, except for two-sample *t*-tests. This procedure is free from assumptions about the distributions (e.g. Student *t* for *R*-values), which are typically violated in small sample sizes[65]. Scatterplots were visualized with 95% confidence bounds (gray or light-red areas).

Reporting summary. Further information on research design is available in the Nature Research Reporting Summary linked to this article.

Data availability

The DBS MRI datasets generated during and analyzed during the current study are not publicly available due to data privacy regulations of patient data but are available from the corresponding author upon reasonable request. The resulting tract atlas is openly available within Lead-DBS software (www.lead-dbs.org).

Code availability

All code used to analyze the dataset is openly available within Lead-DBS/-Connectome software (https://github.com/leaddbs/leaddbs).

Received: 13 April 2019; Accepted: 21 May 2020;
Published online: 03 July 2020

References

1. Ruscio, A. M., Stein, D. J., Chiu, W. T. & Kessler, R. C. The epidemiology of obsessive-compulsive disorder in the National Comorbidity Survey Replication. *Mol. Psychiatry* **15**, 53–63 (2010).
2. Anderson, D. & Ahmed, A. Treatment of patients with intractable obsessive—compulsive disorder with anterior capsular stimulation: case report. *J. Neurosurg.* **98**, 1104–1108 (2003).
3. Mallet, L. et al. Compulsions, Parkinson's disease, and stimulation. *Lancet* **360**, 1302–1304 (2002).
4. Chabardès, S. et al. Deep brain stimulation for obsessive-compulsive disorder: subthalamic nucleus target. *World Neurosurg.* **80**, S31.e1–S31.e8 (2013).
5. Sturm, V. et al. The nucleus accumbens: a target for deep brain stimulation in obsessive–compulsive- and anxiety-disorders. *J. Chem. Neuroanat.* **26**, 293–299 (2003).
6. Greenberg, B. D. et al. Three-year outcomes in deep brain stimulation for highly resistant obsessive–compulsive disorder. *Neuropsychopharmacology* **31**, 2384–2393 (2006).

7. Jiménez-Ponce, F. et al. Preliminary study in patients with obsessive-compulsive disorder treated with electrical stimulation in the inferior thalamic peduncle. *Oper. Neurosurg.* **65**, ons203–ons209 (2009).
8. Luyten, L., Hendrickx, S., Raymaekers, S., Gabriëls, L. & Nuttin, B. Electrical stimulation in the bed nucleus of the stria terminalis alleviates severe obsessive-compulsive disorder. *Mol. Psychiatry* **21**, 1272–1280 (2016).
9. Nair, G., Evans, A., Bear, R. E., Velakoulis, D. & Bittar, R. G. The anteromedial GPi as a new target for deep brain stimulation in obsessive compulsive disorder. *J. Clin. Neurosci.* **21**, 815–821 (2014).
10. Coenen, V. A. et al. The medial forebrain bundle as a target for deep brain stimulation for obsessive-compulsive disorder. *CNS Spectr.* **22**, 282–289 (2017).
11. Maarouf, M. et al. Deep brain stimulation of medial dorsal and ventral anterior nucleus of the thalamus in OCD: a retrospective case series. *PLoS ONE* **11**, e0160750 (2016).
12. Borders, C., Hsu, F., Sweidan, A. J., Matei, E. S. & Bota, R. G. Deep brain stimulation for obsessive compulsive disorder: A review of results by anatomical target. *Ment. Illn.* **10**, 7900 (2018).
13. Tyagi, H. et al. A randomized trial directly comparing ventral capsule and anteromedial subthalamic nucleus stimulation in obsessive-compulsive disorder: clinical and imaging evidence for dissociable effects. *Biol. Psychiatry* https://doi.org/10.1016/j.biopsych.2019.01.017 (2019).
14. Choi, K. S., Riva-Posse, P., Gross, R. E. & Mayberg, H. S. Mapping the "Depression Switch" during intraoperative testing of subcallosal cingulate deep brain stimulation. *JAMA Neurol.* **72**, 1252–1260 (2015).
15. Riva-Posse, P. et al. A connectomic approach for subcallosal cingulate deep brain stimulation surgery: prospective targeting in treatment-resistant depression. *Mol. Psychiatry* **23**, 843–849 (2018).
16. Henderson, J. M. M. D. "Connectomic surgery": diffusion tensor imaging (DTI) tractography as a targeting modality for surgical modulation of neural networks. *Front. Integr. Neurosci.* **6**, 15 (2012).
17. Petersen, M. V. et al. Holographic reconstruction of axonal pathways in the human brain. *Neuron* **104**, 1056–1064.e3 (2019).
18. Feldman, R. P. & Goodrich, J. T. Psychosurgery: a historical overview. *Neurosurgery* **48**, 647–659 (2001).
19. Coenen, V. A., Allert, N. & Mädler, B. A role of diffusion tensor imaging fiber tracking in deep brain stimulation surgery: DBS of the dentato-rubro-thalamic tract (drt) for the treatment of therapy-refractory tremor. *Acta Neurochir.* **153**, 1579–1585 (2011).
20. Schlaepfer, T. E., Bewernick, B. H., Kayser, S., Hurlemann, R. & Coenen, V. A. Deep Brain Stimulation of the Human Reward System for Major Depression—Rationale, Outcomes and Outlook. *Neuropsychopharmacology* **39**, 1303–1314 (2014).
21. Heilbronner, S. R., Safadi, Z. & Haber, S. N. in *Neuromodulation in Psychiatry* (eds. Hamani, C., Lozano, A., Holtzheimer, P. & Mayberg, H.) 27–48 (John Wiley & Sons, Ltd, 2016).
22. Horn, A. et al. Connectivity predicts deep brain stimulation outcome in Parkinson disease. *Ann. Neurol.* **82**, 67–78 (2017).
23. Irmen, F. et al. Left Prefrontal Connectivity Links Subthalamic Stimulation with Depressive Symptoms. *Ann. Neurol.* **87**, 962–975 (2020).
24. Baldermann, J. C. et al. Connectivity profile predictive of effective deep brain stimulation in obsessive compulsive disorder. *Biol. Psychiatry* https://doi.org/10.1016/j.biopsych.2018.12.019 (2019).
25. Akram, H. et al. Subthalamic deep brain stimulation sweet spots and hyperdirect cortical connectivity in Parkinson's disease. *NeuroImage* **158**, 332–345 (2017).
26. Vanegas-Arroyave, N. et al. Tractography patterns of subthalamic nucleus deep brain stimulation. *Brain* **139**, 1200–1210 (2016).
27. Vissani, M. et al. Spatio-temporal structure of single neuron subthalamic activity identifies DBS target for anesthetized Tourette syndrome patients. *J. Neural Eng.* **16**, 066011 (2019).
28. Alkemade, A., Groot, J. M. & Forstmann, B. U. Do we need a human post mortem whole-brain anatomical ground truth in in vivo magnetic resonance imaging? *Front. Neuroanat.* **12**, 110 (2018).
29. Polosan, M. et al. Affective modulation of the associative-limbic subthalamic nucleus: deep brain stimulation in obsessive–compulsive disorder. *Transl. Psychiatry* **9**, 73 (2019).
30. Barcia, J. A. et al. Personalized striatal targets for deep brain stimulation in obsessive-compulsive disorder. *Brain Stimul.* https://doi.org/10.1016/j.brs.2018.12.226 (2018).
31. Maier-Hein, K. H. et al. The challenge of mapping the human connectome based on diffusion tractography. *Nat. Commun.* **8**, 1349 (2017).
32. Horn, A. et al. Probabilistic conversion of neurosurgical DBS electrode coordinates into MNI space. *NeuroImage* **150**, 395–404 (2017).
33. Haynes, W. I. A. & Haber, S. N. The organization of prefrontal-subthalamic inputs in primates provides an anatomical substrate for both functional specificity and integration: implications for basal ganglia models and deep brain stimulation. *J. Neurosci.* **33**, 4804–4814 (2013).
34. Nieuwenhuys, R., Voogd, J. & van Huijzen, C. *The Human Central Nervous System* (Springer, Berlin, 2008).
35. McIntyre, C. C. & Hahn, P. J. Network perspectives on the mechanisms of deep brain stimulation. *Neurobiol. Dis.* **38**, 329–337 (2010).
36. Nambu, A., Tokuno, H. & Takada, M. Functional significance of the cortico–subthalamo–pallidal 'hyperdirect' pathway. *Neurosci. Res.* **43**, 111–117 (2002).
37. Coenen, V. A. et al. Surgical decision making for deep brain stimulation should not be based on aggregated normative data mining. *Brain Stimul.* **12**, 1345–1348 (2019).
38. Nougaret, S., Meffre, J., Duclos, Y., Breysse, E. & Pelloux, Y. First evidence of a hyperdirect prefrontal pathway in the primate: precise organization for new insights on subthalamic nucleus functions. *Front. Comput. Neurosci.* **7**, 135 (2013).
39. Chudasama, Y., Baunez, C. & Robbins, T. W. Functional disconnection of the medial prefrontal cortex and subthalamic nucleus in attentional performance: evidence for corticosubthalamic interaction. *J. Neurosci.* **23**, 5477–5485 (2003).
40. McGovern, R. A. & Sheth, S. A. Role of the dorsal anterior cingulate cortex in obsessive-compulsive disorder: converging evidence from cognitive neuroscience and psychiatric neurosurgery. *J. Neurosurg.* **126**, 132–147 (2017).
41. Dougherty, D. D. et al. Prospective long-term follow-up of 44 patients who received cingulotomy for treatment-refractory obsessive-compulsive disorder. *Am. J. Psychiatry* **159**, 269–275 (2002).
42. Schilling, K. G. et al. Challenges in diffusion MRI tractography—lessons learned from international benchmark competitions. *Magn. Reson. Imaging* **57**, 194–209 (2019).
43. Parent, A. & Hazrati, L.-N. Functional anatomy of the basal ganglia. II. The place of subthalamic nucleus and external pallidium in basal ganglia circuitry. *Brain Res. Rev.* **20**, 128–154 (1995).
44. Coenen, V. A. et al. Tractographic description of major subcortical projection pathways passing the anterior limb of the internal capsule. Corticopetal organization of networks relevant for psychiatric disorders. *NeuroImage Clin.* **25**, 102165 (2020).
45. Liebrand, L. C. et al. Individual white matter bundle trajectories are associated with deep brain stimulation response in obsessive-compulsive disorder. *Brain Stimul.* **12**, 353–360 (2019).
46. Safadi, Z. et al. Functional segmentation of the anterior limb of the internal capsule: linking white matter abnormalities to specific connections. *J. Neurosci.* **38**, 2106–2117 (2018).
47. Mataix-Cols, D. et al. Distinct neural correlates of washing, checking, and hoarding symptom dimensions in obsessive-compulsive disorder. *Arch. Gen. Psychiatry* **61**, 564–576 (2004).
48. Al-Fatly, B. et al. Connectivity profile of thalamic deep brain stimulation to effectively treat essential tremor. *Brain* https://doi.org/10.1093/brain/awz236 (2019).
49. Mayberg, H. S. et al. Deep brain stimulation for treatment-resistant depression. *Neuron* **45**, 651–660 (2005).
50. Schlaepfer, T. E., Bewernick, B. H., Kayser, S., Mädler, B. & Coenen, V. A. Rapid effects of deep brain stimulation for treatment-resistant major depression. *Biol. Psychiatry* **73**, 1204–1212 (2013).
51. Odekerken, V. J. J. et al. GPi vs STN deep brain stimulation for Parkinson disease: three-year follow-up. *Neurology* **86**, 755–761 (2016).
52. Van Essen, D. C. et al. The WU-Minn human connectome project: an overview. *NeuroImage* **80**, 62–79 (2013).
53. Darby, R. R., Horn, A., Cushman, F. & Fox, M. D. Lesion network localization of criminal behavior. *Proc. Natl Acad. Sci. USA* **115**, 601–606 (2018).
54. Joutsa, J. et al. Identifying therapeutic targets from spontaneous beneficial brain lesions. *Ann. Neurol.* **84**, 153–157 (2018).
55. Weigand, A. et al. Prospective validation that subgenual connectivity predicts antidepressant efficacy of transcranial magnetic stimulation sites. *Biol. Psychiatry* **84**, 28–37 (2018).
56. Petersen, M. V. et al. Probabilistic versus deterministic tractography for delineation of the cortico-subthalamic hyperdirect pathway in patients with Parkinson disease selected for deep brain stimulation. *J. Neurosurg.* **126**, 1657–1668 (2017).
57. Jakab, A. et al. Feasibility of diffusion tractography for the reconstruction of intra-thalamic and cerebello-thalamic targets for functional neurosurgery: a multi-vendor pilot study in four subjects. *Front. Neuroanat.* **10**, 76 (2016).
58. Horn, A. et al. Lead-DBS v2: towards a comprehensive pipeline for deep brain stimulation imaging. *NeuroImage* **184**, 293–316 (2019).
59. Husch, A., V. Petersen, M., Gemmar, P., Goncalves, J. & Hertel, F. PaCER—a fully automated method for electrode trajectory and contact reconstruction in deep brain stimulation. *NeuroImage Clin.* **17**, 80–89 (2017).
60. Ewert, S. et al. Optimization and comparative evaluation of nonlinear deformation algorithms for atlas-based segmentation of DBS target nuclei. *NeuroImage* **184**, 586–598 (2019).

61. Schönecker, T., Kupsch, A., Kühn, A. A., Schneider, G.-H. & Hoffmann, K.-T. Automated optimization of subcortical cerebral mr imaging-atlas coregistration for improved postoperative electrode localization in deep brain stimulation. *Am. J. Neuroradiol.* **30**, 1914–1921 (2009).
62. Avants, B. B., Tustison, N. & Song, G. Advanced normalization tools (ANTS). *Insight J.* **2**, 1–35 (2009).
63. Pauli, W. M., Nili, A. N. & Tyszka, J. M. A high-resolution probabilistic in vivo atlas of human subcortical brain nuclei. *Sci. Data* **5**, 180063 (2018).
64. Ewert, S. et al. Toward defining deep brain stimulation targets in MNI space: A subcortical atlas based on multimodal MRI, histology and structural connectivity. *NeuroImage* **170**, 271–282 (2018).
65. Good, P. I. *Permutation, Parametric, and Bootstrap Tests of Hypotheses* (Springer-Verlag, 2005).
66. Mallet, L. et al. Subthalamic nucleus stimulation in severe obsessive–compulsive disorder. *N. Engl. J. Med.* **359**, 2121–2134 (2008).
67. Tsai, H.-C., Chen, S.-Y., Tsai, S.-T., Hung, H.-Y. & Chang, C.-H. Hypomania Following bilateral ventral capsule stimulation in a patient with refractory obsessive-compulsive disorder. *Biol. Psychiatry* **68**, e7–e8 (2010).
68. Nuttin, B. J. et al. Long-term electrical capsular stimulation in patients with obsessive-compulsive disorder. *Neurosurgery* **52**, 1263–1274 (2003).
69. Lee, D. J. et al. Inferior thalamic peduncle deep brain stimulation for treatment-refractory obsessive-compulsive disorder: a phase 1 pilot trial. *Brain Stimul.* **12**, 344–352 (2019).
70. Nuttin, B. et al. Targeting bed nucleus of the stria terminalis for severe obsessive-compulsive disorder: more unexpected lead placement in obsessive-compulsive disorder than in surgery for movement disorders. *World Neurosurg.* **80**, S30.e11–S30.e16 (2013).

Acknowledgements

We would like to thank Kristy Kultas-Ilinsky and Igor Ilinsky, Rudolf Nieuwenhuys and Suzanne Haber for counseling regarding the anatomical validity of tractography results presented in this study. We would like to thank Hagai Bergmann, Helen Mayberg, Paul Krack, Christian Moll, Todd Herrington, Eduardo Alho and Erich Fonoff for very helpful general advice and feedback related to the present work. We would like to thank Cyril Pernet, Wolf-Julian Neumann and Roxanne Lofredi for statistical consultation and help on the manuscript. This work was supported by the German Research Foundation (Deutsche Forschungsgemeinschaft, Emmy Noether Stipend 410169619 to A.H., SPP 0141 to A.A.K. and KFO 219 to J.K.). The study was further funded by the Deutsche Forschungsgemeinschaft (DFG, German Research Foundation) – Project-ID 424778381 – TRR 295. We acknowledge support from the German Research Foundation (DFG) and the Open Access Publication Fund of Charité – Universitätsmedizin Berlin. Data were provided in part by the Human Connectome Project, WU-Minn Consortium (principal investigators: David Van Essen and Kamil Ugurbil; 1U54MH091657) funded by the 16 NIH Institutes and Centers that support the NIH Blueprint for Neuroscience Research; and by the McDonnell Center for Systems Neuroscience at Washington University.

Author contributions

N.L. and A.H. conceptualized the study. N.L. and A.H. developed the software pipeline used, analyzed data and wrote the manuscript. J.C.B. conceptualized the study, acquired patient data and revised the manuscript. S.T. performed literature analyses and wrote the manuscript. H.A. acquired and processed patient data and revised the manuscript. G.J.B.E., A.B., and A.M.L. processed and analyzed human connectome data and revised the manuscript. B.A.-F. processed patient data, conceptualized part of the study and revised the manuscript. A.K., B.S., J.A.B., L.Z., E.J., S.C., V.V.-V., M.P., J.K. and A.A.K. acquired patient data and revised the manuscript.

Competing interests

A.M.L. is consultant for Medtronic, Abbott and Boston Scientific. S.C. is consultant for Medtronic, Boston Scientific and Zimmer Biomet. M.P. has received honoraria for lecturing from the Movement Disorder Society, Medtronic, research support from Boston Scientific. J.K. has received financial support for investigator-initiated trials from Medtronic. A.A.K. reports personal fees and non-financial support from Medtronic, personal fees from Boston Scientific, grants and personal fees from Abbott outside the submitted work. A.H. reports lecture fees for Medtronic and Boston Scientific. N.L., J.C.B., A.K., S.T., H.A., G.J.B.E., A.B., B.A.-F., B.S., J.A.B., L.Z., E.J. and V.V.-V. have nothing to disclose.

Additional information

Supplementary information is available for this paper at https://doi.org/10.1038/s41467-020-16734-3.

Correspondence and requests for materials should be addressed to N.L.

Peer review information *Nature Communications* thanks Burkhard Mädler, Guido van Wingen and the other, anonymous, reviewer(s) for their contribution to the peer review of this work. Peer reviewer reports are available.

Reprints and permission information is available at http://www.nature.com/reprints

Publisher's note Springer Nature remains neutral with regard to jurisdictional claims in published maps and institutional affiliations.

Curriculum Vitae

My curriculum vitae does not appear in the electronic version of my paper for reasons of data protection.

Acknowledgements

It has been a long journey to come to the end of my doctoral study. I have been very grateful that there are always very nice people around me along this journey, without whom it would not be possible for me to complete my study.

I would like to express my deep gratitude to my principal supervisor Dr. Andreas Horn for his enthusiasm, encouragement, guidance, support, and patience. I have been very fortunate and pleased to work with him since long. I have learned a lot from his mentoring. I would also like to sincerely thank my second supervisor Prof. Andrea Kühn for offering me the opportunity to work in such an exciting multidisciplinary team and all her supports.

I would like to acknowledge the data sharing, the valuable input, the constant support, and patience of all the collaborators on my publications.

I would like to thank all my colleagues and friends in the lab. It has been a great pleasure working with them. I very much appreciate the input and contribution of Svenja Treu, Bassam Al-Fatly and Barbara Hollunder to my publications. Thanks to Barbara Hollunder for proofreading my dissertation.

I would also like to acknowledge the support from DAAD, which made it possible for me to start my journey in Germany.

Finally, I would like to give my heartfelt thanks to my parents, my sister, and my wife. Their love, care and support have been motivating me all the time and providing me endless power. My special thanks also go to my daughter for bringing me so much happiness.